ARMY RESEARCH LABORATORY

The Vibrational Stiffness of an Atomic Lattice

by Steven B. Segletes

ARL-TR-1757 September 1998

The findings in this report are not to be construed as an official Department of the Army position unless so designated by other authorized documents.

Citation of manufacturer's or trade names does not constitute an official endorsement or approval of the use thereof.

Destroy this report when it is no longer needed. Do not return it to the originator.

ERRATUM SHEET

re: ARL-TR-1757, "The Vibrational Stiffness of an Atomic Lattice," by Steven B. Segletes

Request the following change be made to subject report:

The notations on Figure 1b (page 21) reflect slightly incorrect values for the lattice and pairwise stiffness. The correct values are 4.55 and 4.82, respectively. A corrected figure is provided (attached hereto). Request corrected figure be cut and pasted into report.

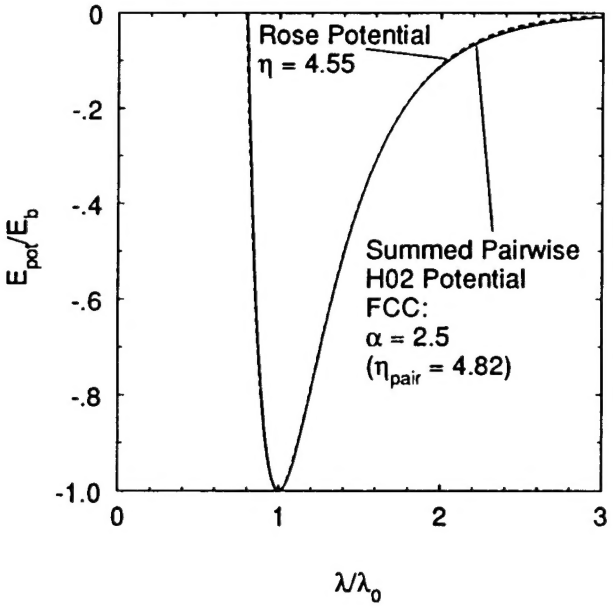

SEGLETES FIG 1R

Army Research Laboratory
Aberdeen Proving Ground, MD 21005-5066

ARL-TR-1757 **September 1998**

The Vibrational Stiffness of an Atomic Lattice

Steven B. Segletes
Weapons and Materials Research Directorate, ARL

Abstract

A static-atomic model is described, which may be employed to evaluate the characteristic vibrational stiffness of an atomic lattice, given the pair-wise potential of the constituent atom. Because the vibrational stiffness is directly related to the resultant vibrational frequency spectrum of the lattice, the method may be used to infer the behavior of the characteristic lattice frequency as a function of lattice spacing. The characteristic frequency behavior is sufficient to determine the Grüneisen function, an important thermodynamic parameter relating to thermal behavior of a crystal lattice. The current method computes and utilizes several spring constants derived from a static lattice in order to infer the characteristic vibrational behavior. No atomic dynamics calculations involving either the equations of motion or modal (vibrational) analysis are required. As such, the method generally requires mere seconds of computation on today's generation of desktop workstations. Results indicate that the vibrational stiffness of the lattice is qualitatively distinct from the volumetric stiffness of the lattice, and, furthermore, that the resulting lattice behavior can be described, over a wide region of lattice spacing, by an analytical equation of state in terms of lattice frequency.

Acknowledgments

The author would like to thank several people who have had a direct hand in improving this report. Dr. Andrew Dietrich of the U.S. Army Research Laboratory (ARL), through his many technical discussions, has permitted the author to more fully appreciate the breadth and nuances of the lattice-vibration problem. Dr. William P. Walters, also of ARL, made a number of valuable suggestions in the course of providing a thorough technical review of the work, for which the author is grateful. Mr. Eric Edwards, of LB&B, has provided yet another outstanding editorial review, as he has done on many other occasions in the past. The interactions with all of these individuals have made this report a more thorough, more accurate, and more readable document. The author would lastly give eternal thanks to his wife, Gabriele, who has provided complete support in all of the author's endeavors.

INTENTIONALLY LEFT BLANK.

Table of Contents

INTENTIONALLY LEFT BLANK.

List of Figures

List of Tables

INTENTIONALLY LEFT BLANK.

PART I—A Static Atomic Paradigm for Lattice Vibration

1. Introduction

The determination of the vibrational behavior of a crystal lattice is fundamental to the understanding of the thermal behavior of crystalline materials. The magnitude and distribution of the lattice's vibrational spectrum was, for example, a key ingredient in the development of plausible specific-heat models by Debye; Born and von Karman [1]; and others early this century. Whereas the specific heat, C_V, relates the behavior of thermal energy and temperature at constant volume, V, it is the Grüneisen function, Γ, macroscopically given by $\Gamma = -V(\partial p_{th}/\partial E_{th})_V$, that relates the behavior of a lattice's thermal energy, E_{th}, to the thermal pressure, p_{th}, at constant volume.

At the atomic level, there is contribution to the Grüneisen function, Γ_i, associated with each mode of the lattice's vibrational spectrum, which is given by $\Gamma_i = -V(\partial \nu_i/\partial V)_T/\nu_i$, where ν_i denotes a frequency component of the vibrational spectrum. Historically [2], attempts to aggregate the Γ_i components into a macroscopic value for Γ were accomplished with the use of two assumptions: (1) that the frequency spectrum took on a particular idealized form (*e.g.*, that of Debye); and (2) that the behavior of every ν_i component changed with volume in a characteristically similar manner. With these assumptions, knowledge of the behavior of the lattice's characteristic frequency alone (and not the details of the vibrational spectrum) is sufficient to determine the macroscopic value for Γ, as $\Gamma = -V(\partial\omega/\partial V)_T/\omega$, where ω is the characteristic frequency of the lattice, rather than a constituent component of the spectrum. With the use of one further assumption, generally supported by data, that Γ is independent of temperature, T, the definition for the Grüneisen function may be alternately given as

$$1/\psi = \Gamma/V = -(d\omega/dV)/\omega \quad , \tag{1–1}$$

where ψ is introduced in this equation as a definition. Since ω is constant ($d\omega/dV$ is zero) for

the special case of a harmonic lattice, Γ may also be thought of as a measure of the lattice's vibrational anharmonicity.

More recently, Plendl [3, 4] analyzed actual, rather than idealized, frequency spectra. Through extensive correlation, he quantitatively determined that the characteristic frequency of any given atomic vibrational spectrum could be computed by the center of gravity of that spectrum, the so-called centro-frequency, as in

$$\omega = \nu_{ctr} = \frac{\int_0^\infty \nu f(\nu)\, d\nu}{\int_0^\infty f(\nu)\, d\nu} , \qquad (1\text{–}2)$$

where ν_{ctr} is the centro-frequency, and $f(\nu)$ is the experimentally measured frequency spectrum. That the characteristic frequency, ω, may be given by ν_{ctr} is telling. It says that the actual spectrum must straddle the characteristic frequency, unlike, for example, the idealized Debye spectrum in which the characteristic frequency is the largest frequency component of the spectrum. More specifically, the characteristic frequency is a weighted average of the frequency spectrum. This concept is of some importance to subsequent discussions on the nature of the characteristic lattice stiffness.

2. Previous Models of the Grüneisen Function

A number of models have been introduced for the calculation of Γ. An early model, of Slater [2], examined the restoring force upon an atom displaced from its rest position in the lattice and used this to determine a spring constant and thus a frequency. However, because Slater quantified the spring constant in terms of pressure-volume compressibility, rather than an interatomic force-displacement relation, his formula could not recreate the proper value of $\Gamma = 0$ for the limiting harmonic case. Dugdale and MacDonald [5] remedied this deficiency by using

the properly constructed spring constant. However, in both of these analyses, only nearest-neighbor interactions were considered and only longitudinal waves were modeled.

Later, Pastine [6] and Vashchenko and Zubarev [7] introduced separate models for Γ, which tried to improve on prior work by accounting for transverse waves, in addition to the longitudinal waves considered in earlier works. Both these works relied on the characterization of empirically composed, volume-dependent Poisson ratios, the theoretical basis for which was no better understood than that for Γ, unfortunately. In the case of Vashchenko and Zubarev, however, the empirical function was chosen in such a manner as to reproduce, for three special cases, the models of Slater, Dugdale and MacDonald, and the free volume theory, respectively.

Common to these and other analyses [2, 5, 8, 9] was the assumption that the volumetric stiffness of the lattice, proportional to the second derivative of the energy potential with respect to lattice spacing, $d^2E_{pot}/d\lambda^2$, is proportional to the vibrational stiffness of the lattice. Such an assumption has been pervasive for two reasons: (1) for a harmonic lattice, it is strictly true; and (2) when only nearest-neighbor interactions are considered for the case of infinitesimal vibrational amplitudes, it is true by virtue of linearization. These two assumptions cover a wide range of modeling strategies, as the only alternative would seem to be the modeling of nonlinear effects and non-nearest-neighbor interactions, with the resultant set of coupled, nonlinear equations being solvable through numerical means only (*e.g.*, time integration or modal analysis).

Recently, Segletes [10] proposed a semi-empirical equation of state that accurately describes the lattice force and vibrational stiffness for many metals to several megabars of pressure, in terms of the vibrational frequency of the lattice. In this model, the zero-temperature lattice force varies as

$$F = (C_0/\Gamma_0)^2 \cdot \lambda^2/\psi \cdot (\omega/\omega_0)^K \ln(\omega/\omega_0) \quad , \tag{2–1}$$

where the "0" subscript denotes conditions at the reference, zero-force state, C_0 is the bulk sound speed at the reference state, and K, taken as a constant $K = \eta/(3\Gamma_0)$, indicates a ratio of

volumetric to vibrational anharmonicity (where η is a nondimensional parameter employed by Rose *et al.* [11]), which correlates the curvature of the lattice potential (*i.e.*, the slope of the force) at the reference state to the binding energy of the lattice potential. The variable λ is the current lattice spacing, and ψ, as defined in eqn (1–1), is simply the ratio V/Γ. The lattice force, F, is characterized by $p_c \lambda^2$, where p_c is the zero-temperature (so-called cold) pressure in the lattice. Subsequent analysis of this equation-of-state form [12–14] revealed that the volumetric stiffness of the lattice, denoted $dF/d\lambda$, was of a different functional form than the vibrational stiffness of the lattice, denoted $\partial F_{vib}/\partial x$. In particular, for vibrations of infinitesimal amplitude (which we assume for the low temperature behavior of solids), the vibrational stiffness, from considerations of a linearized vibration analysis, varies as

$$-\partial F_{vib}/\partial x \sim \omega^2 \quad . \tag{2–2}$$

But rather than the volumetric stiffness following this same functional form, a more complicated expression arises from eqn (2–1), which, even when idealized to a quasi-harmonic form, varies instead along the lines of

$$-dF/d\lambda \sim \omega\,[\,\ln(\omega/\omega_0) + 1\,] \qquad \text{(quasi-harmonic)}. \tag{2–3}$$

This disparity provoked speculation that: (1) the omission of non-nearest-neighbor interactions from the early analyses may have led to a systematic error, and (2) there might be some hope of capturing the interactions of nonnearest neighbors within the context of an analytical form along the lines of eqn (2–1).

It is the primary intent of this report to quantitatively analyze the influence of non-nearest-neighbor interactions on various stiffnesses of the lattice, in hopes of ascertaining whether or not there is any basis for the distinction cited between eqns. (2–2) and (2–3), which might lead to a relation like eqn (2–1). To compute the details of the vibrational spectrum, a modal analysis or time-integrated dynamic solution would need to be performed on a large array of lattice atoms. But since only the characteristic frequency is desired, which is sufficent to obtain a value for Γ, we seek a shortcut to the full dynamic solution. Unlike Slater [2] and Dugdale and

MacDonald [5], the current analysis considers the behavior of both the longitudinal and transverse stiffnesses. However, it does so along only the primary axes of the crystal. A contemplated future effort will work to address this limitation. Finally, the method to be proposed here uses a given interatomic pairwise potential (energy *vs.* distance) in order to infer the characteristic frequency behavior of the lattice. It therefore goes without saying that the validity of any results obtained here is bounded by the domain of applicability of the selected potential. We intend to show that, in spite of ignoring directional variations in crystalline behavior, a meaningful description of the characteristic frequency of the lattice can, nonetheless, be obtained.

3. Non-Nearest-Neighbor Interactions

One may argue, for several reasons, that the vibrational and volumetric stiffnesses of an atomic lattice are not functionally equivalent. One compelling argument [13, 14] may be made by considering a one-dimensional string of atoms. The volumetric stiffness quantifies the resultant change of externally applied force required to alter the spacing between every adjacent atom in the lattice by an amount $d\lambda$, whereas the vibrational stiffness quantifies the restoring force on a single atom in question when it, as part of a moving wave, is displaced a distance dx with respect to a lattice that otherwise remains, on average, at a fixed location. In the former case, the resultant change in separation to the n'th nearest neighbor is $n\,d\lambda$, while in the latter case, it is merely dx. Clearly, these two situations, and thus the two associated stiffnesses, must be different if interactions are considered for neighbors $n > 1$. Furthermore, Plendl [3, 4] has actually reported experimental data on this distinction, by comparing his centro-frequency (a measure of vibrational stiffness) to the so-called ''definite frequency'' (a measure of volumetric stiffness) at the equilibrium states for many ionic crystals. He noted that the interrelation of these two frequencies could be characterized in terms of the lattice's exponent of repulsion and they were observed to vary from each other by as much as ±20%.

If one considers a single, infinitesimal wave of disturbance along the principal axis of a crystal lattice, then the characteristic vibrational stiffness of the lattice may be acquired by finding the restoring force on one atom of interest (atom O) by moving a plane of atoms

containing O a distance dx with respect to *an otherwise stationary lattice*. If the displacement, dx, is perpendicular to the plane of atoms, the vibration is a longitudinal one. If dx is parallel with the plane, the vibration is transverse. If knowledge of the characteristic stiffness behavior can be obtained in this manner, then vibration theory for infinitesimal vibrations [*i.e.*, eqn (2–2)] will immediately yield the characteristic vibrational frequency behavior.

For the more realistic case of finite vibrational amplitudes and multiwave disturbances, the instantaneous interatomic stiffness will vary finitely in time because the instantaneous separation of atoms will be a function of the frequency phase-shift of adjacent, vibrating atoms. The averaged value of this time-dependent stiffness may, thus, no longer be exactly that of the infinitesimal-amplitude single-wave stiffness described in the preceeding text, though we hope the infinitesimal stiffness will still serve as a reasonable approximation. In a dynamic solution, the instantaneous distance between any two atoms (*i.e.*, phase information), because of vibration, will be sometimes larger than and other times smaller than the current equilibrium rest distance. The instantaneous, pairwise stiffness will also fluctuate about this equilibrium value (unless the interaction is harmonic, in which case the stiffness is independent of separation). During the course of the vibration, as the stiffness is locally larger than the current equilibrium stiffness, higher frequency modes tend to be excited, and correspondingly, when the instantaneous stiffness is lower than equilibrium, lower frequency modes are excited. Since a vibration necessarily makes excursions about both sides of the equilibrium point, both higher and lower frequency modes will be excited when anharmonicity exists, as compared with a locally harmonic spectrum.

And yet, the average effect on the centro-frequency of the spectrum may be small by comparison, since the simultaneous introduction of higher and lower frequency modes will tend to cancel out in the centro-frequency calculation of eqn (1–2). So it goes, too, with the vibrational stiffness because of the monotonic relation between frequency and stiffness, eqn (2–2). Thus, while anharmonic effects will cause the pairwise stiffness to fluctuate in time about its equilibrium value for finitely large vibrational amplitudes, it is the static value of that stiffness that might reasonably be used to approximate the time-averaged characteristic stiffness corresponding to the centro-frequency.

In the same way that determination of a spring stiffness, for a simple mass-spring arrangement, is sufficient to characterize the resultant vibrational frequency without having to reevaluate the equations of dynamic motion, we intend to compute and utilize several spring constants derived from a static lattice in order to infer the characteristic vibrational behavior. No atomic dynamics calculations involving either the equations of motion or modal analysis will be required. Essentially, the equation of motion is already contained in the solution represented by eqn (2–2), for a simple spring-mass system under infinitesimal vibrational amplitude.

One other reason to believe that the static stiffness of a lattice may be used to characterize the dynamic solution is that, in a lattice, vibrational amplitude is a measure of temperature. And since Γ is, for actual lattices, generally found to be temperature-insensitive over a large range, we may conclude that the stiffness and its derivatives are vibrational-amplitude insensitive to the same extent.

4. Volumetric Distention

Let $\varepsilon(s)$ denote the energy potential between any two atoms in a 3-D simple-cubic lattice, separated by a distance s. Then f, given by $-d\varepsilon/ds$ (positive in compression), will denote the pairwise force. Considering our atom of interest, atom O, to be at the origin, we use the index ijk to denote an atom located relative to the origin at coordinate $(x, y, z) = (\lambda i, \lambda j, \lambda k)$, where λ is the current lattice spacing of the given simple-cubic lattice. Applying the distance formula, $s_{ijk}^2 = (x^2 + y^2 + z^2)$, from our atom of interest to the atom ijk is simply

$$s_{ijk} = \lambda(i^2 + j^2 + k^2)^{1/2} \quad . \tag{4–1}$$

If we use $E_{pot}(\lambda)$ to denote the summed potential energy for the atom at the origin, arising from the contributions of every other atom in the lattice, then for a lattice of infinite extent with an instantaneous lattice-spacing of λ, we have

$$E_{pot}(\lambda) = \sum_{i=-\infty}^{\infty} \sum_{j=-\infty}^{\infty} \sum_{k=-\infty}^{\infty} \varepsilon(s_{ijk}) \quad , \tag{4–2}$$

where we define $\varepsilon(0) = 0$, to preclude the situation of atom O producing a contribution to its own potential.

If we first consider the case of volumetric expansion, whereby the spacing between adjacent atoms in the lattice is increased from λ to $\lambda + d\lambda$, eqn (4–1) indicates, for a given pair of atoms, that s_{ijk} is directly proportional to λ. Thus, the separation metric between the origin and atom *ijk*, for volumetric expansion, is obtained from eqn (4–1) as

$$ds_{vol}/d\lambda = s_{ijk}/\lambda = (i^2 + j^2 + k^2)^{1/2} \quad . \tag{4–3}$$

Eqn (4–3) merely indicates that the amount of increased separation caused by an incremental change in λ is directly proportional to the distance of *ijk* from *O*. The quantity $ds_{vol}/d\lambda$ is a function only of the topological indices, *i*, *j*, and *k*, and not of λ or *s*. Thus, for any given atom, *ijk*, this metric is constant under volumetric dilatation. As such, higher derivatives, such as $d^2 s_{vol}/d\lambda^2$, are identically zero.

A spring force, in general, is given by $F \sim dE/dx$. By attaching to the term "lattice force" the physical meaning of $p_c \lambda^2$, where p_c is the cold pressure of the lattice, it may be shown, for the current case, that $F = -(dE_{pot}/d\lambda)/3$, consistent with the spring notion. We therefore compute F (physically representing the external unit force required to volumetrically compress the lattice) as

$$F(\lambda) = -1/3 \sum_{i=-\infty}^{\infty} \sum_{j=-\infty}^{\infty} \sum_{k=-\infty}^{\infty} d\varepsilon/d\lambda \Big|_{s_{ijk}} \quad . \tag{4–4}$$

Furthermore, the term $d\varepsilon/d\lambda$, for the case of volumetric expansion, is $d\varepsilon/ds \cdot ds_{vol}/d\lambda$. The first deriviative of the pairwise energy potential is simply the negative of the pairwise force—thus,

$$F(\lambda) = 1/3 \sum_{i=-\infty}^{\infty} \sum_{j=-\infty}^{\infty} \sum_{k=-\infty}^{\infty} f(s_{ijk})\ ds_{vol}/d\lambda\big|_{ijk} \quad . \tag{4–5}$$

We wish to compute the spacial derivative of eqn (4–5) for the case of volumetric deformation, since the force-derivative is itself one of the spring stiffnesses being sought. For the case of volumetric distention, we again take the derivative with respect to λ to obtain

$$dF/d\lambda = 1/3 \sum_{i=-\infty}^{\infty} \sum_{j=-\infty}^{\infty} \sum_{k=-\infty}^{\infty} df/ds\,\big|_{s_{ijk}}\ (ds_{vol}/d\lambda\,\big|_{ijk})^2 \quad . \tag{4–6}$$

With the use of eqn (4–3), eqns (4–5) and (4–6) may be simplified as

$$F = 1/3 \sum_{i=-\infty}^{\infty} \sum_{j=-\infty}^{\infty} \sum_{k=-\infty}^{\infty} f(s_{ijk})\ (i^2 + j^2 + k^2)^{1/2} \tag{4–7}$$

and

$$dF/d\lambda = 1/3 \sum_{i=-\infty}^{\infty} \sum_{j=-\infty}^{\infty} \sum_{k=-\infty}^{\infty} df/ds\,\big|_{s_{ijk}}\ (i^2 + j^2 + k^2) \quad . \tag{4–8}$$

5. Vibrational Distortion (Longitudinal)

In contrast to the situation of volumetric distention, an instantaneous snapshot of the simplest vibrational distortion (*i.e.*, a planar pulse) involves the displacement of a single plane of atoms with respect to an otherwise stationary lattice. Again, consider our atom of interest, *O*,

to be initially located at the origin, at the moment a longitudinal plane wave traveling from the $+x$ direction to the $-x$ direction just passes the origin. At this instant, all atoms in the $x = 0$ plane are displaced a distance dx in the negative x direction, whereas every other atom in the lattice is located at its nominal, undisturbed position. For all atoms in the displaced plane, no change in position occurs with respect to each other, since all atoms in that plane are moving in unison. However, we may compute the vibrational separation metric between atom O and atom ijk not located in the $x = 0$ plane. In terms of the motion of atom O in the x direction, we can quantify the vibrational separation metric by taking the derivative of the atomic separation to atom ijk, $s_{ijk}^2 = (x^2 + y^2 + z^2)$, with respect to x only. We obtain

$$\partial s_{vib} / \partial x = x / s_{ijk} = \cos\gamma \qquad (i \neq 0 \text{ for longitudinal vibrations}), \tag{5–1}$$

where $\cos\gamma$ is the direction cosine between the line of action, from O to ijk, and the vibrational movement along the x axis. For this particular vibrational mode, it is given by $\cos\gamma = i/(i^2 + j^2 + k^2)^{1/2}$. The $i \neq 0$ restriction in eqn (5–1) accounts for the fact that all other atoms in the $x = 0$ plane are moving in unison with atom O, and their vibrational separation metric thus remains zero. Unlike $ds_{vol}/d\lambda$, the vibrational separation metric is not independent of changes in x. Therefore, higher derivatives will need to be computed as well; for example,

$$\partial^2 s_{vib} / \partial x^2 = 1/s_{ijk} - x^2/s_{ijk}^3 = (\sin^2\gamma)/s_{ijk} \qquad (i \neq 0), \tag{5–2}$$

and so on. As a point of note, for the vibrational mode being considered, $\sin\gamma = [(j^2 + k^2)/(i^2 + j^2 + k^2)]^{1/2}$.

The longitudinal vibrational force in the lattice, call it F_L (physically representing the resultant force on the oscillating atom, O), and its derivative may be obtained in a like manner to the volumetric force quantities, though they will differ from the earlier results in that the derivative of ε is taken with respect to the vibrational displacement, x, and not the lattice spacing, λ. The vibrational force and its derivative are thus

$$F_L(\lambda) = \sum_{i=-\infty}^{\infty} \sum_{j=-\infty}^{\infty} \sum_{k=-\infty}^{\infty} f(s_{ijk})\ \partial s_{vib}/\partial x\,|_{ijk} \qquad (i \neq 0)\ , \tag{5–3}$$

and

$$\partial F_L/\partial x = \sum_{i=-\infty}^{\infty} \sum_{j=-\infty}^{\infty} \sum_{k=-\infty}^{\infty} [\ df/ds\,|_{s_{ijk}}\ (\partial s_{vib}/\partial x\,|_{ijk})^2 + f(s_{ijk})\ \partial^2 s_{vib}/\partial x^2\ ] \qquad (i \neq 0)\ . \tag{5–4}$$

Because the sum is performed at the moment when the vibrating atom is instantaneously at its equilibrium position (the origin), the resultant force, F_{vib}, on the atom should be momentarily zero. We see from eqn (5–1) that $\partial s_{vib}/\partial x$ in the $-x$ half-space is opposite in value to the corresponding point in the $+x$ half space. Thus, the sum of eqn (5–3), when taken over the full 3-D space, will indeed be zero. Were the sum to be performed over the $+x$ half-space only, the resulting nonzero value for force would represent the local force being exerted on the $+x$ side of the atom. However, though the net force on an unextended spring is zero, the stiffness of that same spring is not zero. Eqn (5–4) reveals this point to be the case, as the squared term will always yield a positive contribution to the summation. It is with the use of eqns (5–1) and (5–2) that eqns (5–3) and (5–4) may be simplified as

$$F_L = \sum_{i=-\infty}^{\infty} \sum_{j=-\infty}^{\infty} \sum_{k=-\infty}^{\infty} f(s_{ijk})\ \cos\gamma \ \equiv\ 0 \qquad (i \neq 0)\ , \tag{5–5}$$

and

$$\partial F_L/\partial x = \sum_{i=-\infty}^{\infty} \sum_{j=-\infty}^{\infty} \sum_{k=-\infty}^{\infty} [\ df/ds\,|_{s_{ijk}} \cdot \cos^2\gamma + f(s_{ijk})/s_{ijk} \cdot \sin^2\gamma\ ] \qquad (i \neq 0)\ . \tag{5–6}$$

Eqn (5–6) confirms what we know to be true, were the lattice to be composed of harmonic (*i.e.*, linear) springs. That is, when the force-displacement relationship for the constituent springs of a lattice is linear, such that $df/ds = f/s$, the characteristic vibrational stiffness of the lattice is proportional to the stiffness of the component spring. Furthermore, that constant of proportionality is the number of springs acting on the atom.

6. Vibrational Distortion (Transverse)

Like the longitudinal vibration, an instantaneous snapshot of a transverse vibrational distortion also involves the displacement of a single plane of atoms with respect to an otherwise stationary lattice. Again, we consider our atom of interest, O, to be initially located at the origin, at the moment a transverse plane wave traveling from the $+y$ direction to the $-y$ direction just passes the origin. At this instant, all atoms in the $y = 0$ plane are displaced a distance dx in the negative x direction, whereas every other atom in the lattice is located at its nominal, undisturbed position. For all atoms in the displaced plane, no change in position occurs with respect to each other, since all atoms in that plane are moving in unison. However, we may compute the vibrational separation metric between atom O and atom ijk not located in the $y = 0$ plane. The resulting separation metric between O and atom ijk, when our atom of interest is momentarily displaced to coordinate $(-dx,0,0)$, is likewise obtained, in the manner of eqn (5–1), as

$$\partial s_{vib}/\partial x = x/s_{ijk} = \cos\gamma \qquad (j \neq 0 \text{ for transverse vibrations}) \ . \tag{6–1}$$

The transverse-vibrational force in the lattice, call it F_T (physically representing the resultant force on the oscillating atom, O), and its derivative may be obtained in a like manner to the longitudinal-vibrational force quantities. The transverse-vibrational force and its derivative are thus

$$F_T(\lambda) = \sum_{i=-\infty}^{\infty} \sum_{j=-\infty}^{\infty} \sum_{k=-\infty}^{\infty} f(s_{ijk})\ \partial s_{vib}/\partial x_{\ ijk} \qquad (j \neq 0) \ , \tag{6–2}$$

and

$$\partial F_T/\partial x = \sum_{i=-\infty}^{\infty} \sum_{j=-\infty}^{\infty} \sum_{k=-\infty}^{\infty} [\, df/ds\,|_{s_{ijk}} (\partial s_{vib}/\partial x\,|_{ijk})^2 + f(s_{ijk})\, \partial^2 s_{vib}/\partial x^2 \,] \quad (j \neq 0) \ . \quad (6\text{–}3)$$

Like the longitudinal case, the resultant force, F_T, on the atom will be momentarily zero, though the stiffness of that same spring is not zero. We see that the only difference between these and the longitudinal equations is the nature of the summation restriction as to which atoms are moving in unison with atom O. The final results are thus

$$F_T = \sum_{i=-\infty}^{\infty} \sum_{j=-\infty}^{\infty} \sum_{k=-\infty}^{\infty} f(s_{ijk})\, \cos\gamma \equiv 0 \quad (j \neq 0) \ , \quad (6\text{–}4)$$

and

$$\partial F_T/\partial x = \sum_{i=-\infty}^{\infty} \sum_{j=-\infty}^{\infty} \sum_{k=-\infty}^{\infty} [\, df/ds\,|_{s_{ijk}} \cdot \cos^2\gamma + f(s_{ijk})/s_{ijk} \cdot \sin^2\gamma \,] \quad (j \neq 0) \ . \quad (6\text{–}5)$$

One last note regarding transverse vibrations is that transverse waves traveling in the y and z directions will both produce displacements in the x direction, whereas only a longitudinal vibration in the x direction will do so. Thus, there are two possible transverse vibrational components for every longitudinal component. Because of considerations of symmetry, however, both transverse wave components will exhibit characteristic behavior identical to that expressed by eqn (6–5).

7. Vibrational Stiffness (Aggregated) and Its Derivatives

The vibrational spectrum of an actual material is composed of many different modes. It is plain to see that equations developed to this point, for longitudinal and transverse vibrations,

consider only the modes along the principal axes of the lattice. In this current work, we limit the analysis to this restriction, and for two reasons: (1) primarily, for the sake of simplicity; and (2) because past works by Slater [2] and Grüneisen suggest that different vibrational modes vary in a characteristically similar manner under changes in lattice spacing. Though not reported here, we have formulated modified relations to examine other vibrational modes of the lattice. Preliminary results do indicate, to a large extent, a characteristically similar behavior in terms of variation of the modal frequency with lattice spacing. Ideally, we hope in a future effort to integrate analytically all of the vibrational modes into a characteristic stiffness.

Even with the simplification of restricting the study to the principal vibrational modes of the lattice, we still have, at this point, a need to aggregate the one longitudinal and two corresponding transverse vibrational stiffnesses into a net vibrational stiffness quantity. It may be shown from the work of Slater [2] or Brillouin [8] (which presents the result directly) that the frequency components are related to an aggregated frequency by way of

$$3/\omega^3 = 1/\omega_L^3 + 2/\omega_T^3 \quad . \tag{7–1}$$

These frequencies vary with their associated stiffnesses by way of eqn (2–2). Therefore, an aggregated stiffness may be obtained as

$$-\partial F_{vib}/\partial x = \{ 3 / [1/(-\partial F_L/\partial x)^{3/2} + 2/(-\partial F_T/\partial x)^{3/2}] \}^{2/3} \quad . \tag{7–2}$$

Note that even though the longitudinal and transverse components of the vibrational stiffness may change sign (becoming positive) at large extensions of the lattice, eqn (7–2) loses its traditional meaning when either of the component stiffnesses becomes positive, and the calculation may, thus, be abandoned for lattice extensions beyond this point.

Subsequent analysis, in pursuit of the Grüneisen function, will also require the derivative of this aggregated stiffness with respect to lattice spacing, λ. Tedious, but straightforward, differentiation gives

$$\frac{d}{d\lambda}(\partial F_{vib}/\partial x) = 1/3 \cdot \left(\frac{\partial F_{vib}/\partial x}{\partial F_L/\partial x}\right)^{5/2} \frac{d}{d\lambda}(\partial F_L/\partial x) + 2/3 \cdot \left(\frac{\partial F_{vib}/\partial x}{\partial F_T/\partial x}\right)^{5/2} \frac{d}{d\lambda}(\partial F_T/\partial x) \quad . \quad (7\text{–}3)$$

The individual L and T component and aggregated stiffness values may be obtained via eqns (5–6), (6–5), and (7–2), respectively. In addition, derivatives of the component stiffnesses with respect to λ are obtained by taking the derivatives of eqns (5–4) and (6–3) with respect to λ (not x).

Though the angle, γ, between the pairwise force's line of action and the direction of vibration does not vary under volumetric change, the distance s_{ijk} does change according to the separation metric $ds_{vol}/d\lambda$, eqn (4–3). Thus, to accomplish the derivatives of the stiffness components required of eqn (7–3), we make use of the following derivatives of eqns (5–1) and (5–2):

$$d/d\lambda(\partial s_{vib}/\partial x) = 0 \quad , \quad (7\text{–}4)$$

and, referring to eqn (4–3),

$$d/d\lambda(\partial^2 s_{vib}/\partial x^2) = -(\sin^2\gamma)/s_{ijk}^2 \cdot ds_{vol}/d\lambda \quad . \quad (7\text{–}5)$$

With the use of these, the derivatives of eqns (5–4) and (6–3) become

$$\frac{d}{d\lambda}\left(\frac{\partial F_L}{\partial x}\right) = \sum_{i=-\infty}^{\infty}\sum_{j=-\infty}^{\infty}\sum_{k=-\infty}^{\infty} \frac{ds_{vol}}{d\lambda}\left[d^2f/ds^2\,|_{s_{ijk}} \cos^2\gamma + \left(\frac{df/ds\,|_{s_{ijk}}}{s_{ijk}} - \frac{f(s_{ijk})}{s_{ijk}^2}\right)\sin^2\gamma\right]$$

$$(i \neq 0) \quad (7\text{–}6)$$

and

$$\frac{d}{d\lambda}\left(\frac{\partial F_T}{\partial x}\right) = \sum_{i=-\infty}^{\infty}\sum_{j=-\infty}^{\infty}\sum_{k=-\infty}^{\infty}\frac{ds_{vol}}{d\lambda}\left[d^2f/ds^2\Big|_{s_{ijk}}\cos^2\gamma - \left(\frac{df/ds\Big|_{s_{ijk}}}{s_{ijk}} - \frac{f(s_{ijk})}{s_{ijk}^2}\right)\sin^2\gamma\right]$$

$$(j \neq 0) \quad . \qquad (7\text{–}7)$$

It may again be confirmed from these two results that, were the lattice composed of linear (harmonic) springs wherein $df/ds = f/s$ and $d^2f/ds^2 = 0$, the variation of lattice stiffness with λ would be identically zero. These two equations may be inserted into eqn (7–3) to obtain the derivative, with respect to λ, of the aggregated stiffness. Subsequent use may be made of eqns (7–2) and (7–3) to help ascertain the vibrational behavior of the lattice. The availability of aggregated quantities, however, does not preclude analysis in terms of the individual longitudinal and transverse (L and T) components of stiffness, which may be used directly, in lieu of eqns (7–2) and (7–3), respectively.

8. Results and Observations

A study is made of the volumetric and vibrational lattice stiffnesses using the preceeding equations. The lattice structures chosen for study is the simple-cubic (SC), body-centered cubic (BCC), and face-centered cubic (FCC) structures. The sole influence of the BCC and FCC structures on the equations derived above is that i, j, and k necessarily take on the appropriate integer-plus-one-half values in addition to integer values. The method described here could reasonably be extended to other lattice structures as well.

To proceed with the analysis, a pairwise potential, $\varepsilon(s)$, must be specified with energy expressible as a function of separation distance, s, so as to determine the influence of any arbitrary atom (located at lattice location ijk) upon our atom of interest, O, conveniently located at the origin. To this end, we select the so-called H02 model of Schulte and Holzapfel [15], primarily because they noted that their model, in contrast to others, exhibited the proper limiting behavior in strong compression. Though this model was not originally proposed as a pairwise potential, we choose it nonetheless for study. And though we have no assurance that it will do

so, the use of this model as the pairwise potential will allow it to be determined, not only if the functional form of the aggregated crystal lattice potential follows that of the pairwise interaction, but whether the decay rates and dimensions of the many-atomed crystal lattice are similar to those of the corresponding pairwise interaction.

Though $\varepsilon(s)$ is taken in this study to be the H02 model, any suitable potential may be used over its domain of compressive accuracy. The far-field behavior of the potential under large expansions is significant as well since the summations of the lattice quantities are, in theory, taken out to infinite separation. This concern is especially relevant for low decay rates, whereupon the potential decays slowly with increased separation. The concern is not one of absolute convergence, since the number of atoms in the summation at a given separation distance goes only as the square of the separation distance, whereas the potential decays exponentially. Rather, the concern is one of what the actual converged value is; a cursory examination has shown some sensitivity of results to the manner in which the potential decays with separation (*i.e.*, sensitivity to the choice of pairwise potential). However, this sensitivity has been one of value, not of trend.

The H02 potential, being used to describe the pairwise interaction of any two atoms in the lattice, actually characterizes the force interaction instead of the energy potential. Because the H02 potential is being used to characterize the pairwise interaction, rather than the full lattice interaction, we must express the potential in terms of force and distance, rather than pressure and volume (as it was originally given) since, for a pairwise interaction, pressure and volume have no meaning. Since $F = p_c \lambda^2$, the H02 expression, expressed in terms of pairwise force, is

$$f = -s_0 (df/ds)_0 \; x^{-3} (1-x) \exp[\alpha (1-x)] \quad , \tag{8–1}$$

where α is the interaction decay constant of the pairwise system and x is a nondimensional interatomic spacing parameter, given by $x = s/s_0$. The parameter $s_0 (df/ds)_0$ quantifies the force gradient at the equilibrium (zero-force), pairwise spacing, s_0. The pairwise energy, $\varepsilon(s)$, and the

force derivative, *df/ds*, may be directly obtained through integration[†] and differentiation of eqn (8–1), respectively.

This study is performed for a variety of representative values of α, with results being obtained as a function of lattice spacing (*i.e.*, the governing equations are summed for various, closely spaced increments of λ/s_0). Since summations to infinity cannot actually be performed, a suitably large radius of influence, s_{max}, is chosen for the summation in order to obtain convergence (*i.e.*, terms were summed if $s_{ijk} \leq s_{max}$). For typical values of λ and α, values of s_{max} equal to 8 to 11 times s_0 were observed to be sufficient, with the larger s_{max} values corresponding to smaller values of α. Of course, for λ values that might be a small fraction of s_0, the number of summed terms grows rapidly, increasing as $[(s_{max}/s_0)(s_0/\lambda)]^3$. Furthermore, as the pairwise decay rate is successively diminished, such that the effects of far-field influence decay ever more slowly with distance, an increasing number of summation terms are required to achieve convergence at a single highly compressed lattice spacing.

[†] The integration of the H02 force function, eqn (8–1), by standard methods requires an infinite summation, with successive terms going as $x^n/(n \cdot n!)$. For large x, corresponding to large lattice spacings, the number of terms required for convergence and the limits of computer precision make this approach impractical. Therefore, a fit was developed for the offending exponential integral. By making use of the substitution, $w = 1/(\alpha x)$, the problem may be expressed in terms of

$$\int_x^\infty \frac{e^{-\alpha x}\,dx}{x^2} = \alpha \int_0^{1/(\alpha x)} e^{-1/w}\,dw \quad .$$

The fit to this transformed integral has been found to be accurate to within 0.008% over the complete domain $w > 0$ ($0 < x < \infty$). The fit is given by

$$\int_0^w e^{-1/w}\,dw \approx e^{-1/w}\left(w - \ln\left\{1 + w - [w - \ln(1+w)] \cdot \frac{(1 + 3.918w + 2.576w^2)}{(1 + 5.573w + 5.888w^2)}\right\}\right) \quad .$$

The constants in this fit are tailored to minimize the relative error in the so-called second exponential integral, $E_2(x)$. A general treatment of this approach for fitting the exponential integrals, E_n, without the use of fit splicing, may be found in Segletes [27].

A number of general observations that seemed to apply regardless of the value of α were made from the results of the study and are given as follows:

(1) The equilibrium condition for the lattice exhibits a nearest-neighbor separation distance less than that for the pairwise interaction. In particular, the equilibrium spacing of the nearest-neighbor atoms within a lattice, s_{eq}, must always be smaller than the pairwise equilibrium spacing, s_0, since for a lattice at equilibrium, the attraction of the far-field atoms must be exactly balanced by the repulsion of the nearest neighbors. These nearest neighbors, on the other hand, can only be exhibiting repulsion if their separation distance is smaller than the equilibrium, pairwise spacing. Table 1 gives the equilibrium lattice separation as a function of pairwise decay rate for the various lattice structures (SC, BCC, and FCC) when using the H02 potential as the pairwise potential. The geometry of lattice structures other than simple cubic dictates that the interatomic spacing to the nearest neighbor, s_{eq}, is less than the unit cell dimension, λ_0. Thus, while the unit cell dimension may exceed the pairwise-equilibrium spacing, s_0, in the case of BCC and FCC structures, the nearest-neighbor separation distance, s_{eq}, will not do so, and for the aforementioned reasons.

Table 1. Relative Values of Equilibrium Lattice Spacing as a Function of Pairwise Interaction Decay Rate

α	λ_0/s_0 (s_{eq}/s_0)		
	SC	BCC	FCC
1.1	0.13 (0.13)	0.16 (0.14)	0.20 (0.14)
1.5	0.45 (0.45)	0.55 (0.48)	0.69 (0.49)
2	0.65 (0.65)	0.79 (0.69)	1.00 (0.71)
2.5	0.76 (0.76)	0.92 (0.79)	1.15 (0.82)
3	0.83 (0.83)	0.99 (0.86)	1.24 (0.88)
4	0.90 (0.90)	1.06 (0.92)	1.33 (0.94)
5	0.94 (0.94)	1.09 (0.95)	1.37 (0.97)
∞	1.00 (1.00)	$2/3^{1/2}$ = 1.15 (1.00)	$2^{1/2}$ = 1.41 (1.00)

Also, the lower the decay rate, the higher the equilibrium compaction (*i.e.*, small α implies small λ_0/s_0). The reason for this behavior is that a smaller exponential decay rate in the potential implies a larger number of far-field neighbors exerting a significant attractive force. This increased attractive force from the far field must be balanced by a larger repulsion from the nearest neighbors. This far-field attraction, therefore, causes the equilibrium lattice spacing, λ_0, to compress significantly with respect to the pairwise equilibrium distance, s_0. For these low-decay-rate cases, the form of the pairwise potential is exercised at both the repulsive and compressive limits of accuracy. The low values of λ_0/s_0 drive the nearest neighbor into an extremely compressed state, while at the same time, the low decay rate allows for significant pairwise interactions from atoms located a far distance away. The number of atoms playing a significant role in the equilibrium calculation will continue to increase as the interaction decay constant is decreased, with the computational burden increasing correspondingly. But such behavior is only a limiting case, and, in general, a complete and converged analysis for a given value of α, over an extensive range of λ, requires mere seconds of computation on today's generation of scientific workstations (*e.g.*, SGI Octane).

(2) The summed lattice force, *F*, like the given pairwise force, *f*, may be nominally described over a moderate range of lattice spacings by the H02 lattice potential of Schulte and Holzapfel [15], with α for the lattice taken identically to the pairwise interaction. There was no reason to have assumed, *a priori*, that the summed potential would take on a similar functional form to the pairwise potential composing it. Table 1, for example, has already indicated that the absolute minimum of the summed potential occurs at a different lattice spacing than the pairwise potential. Nonetheless, it was observed that, up to moderate compressions (*e.g.*, for energies near and below the binding energy), the lattice force follows a similar functional form to the pairwise force, including behavior according to an identical decay constant (*i.e.*, the value for α characterizing the lattice appears to be identical to that characterizing the pairwise interaction). At very high compressions (and particularly for larger values of α), the scaled pairwise- and lattice-force may begin to diverge slightly. Figure 1a shows, in nondimensional terms, the pairwise- and lattice-force for an FCC lattice with $\alpha = 2.5$.

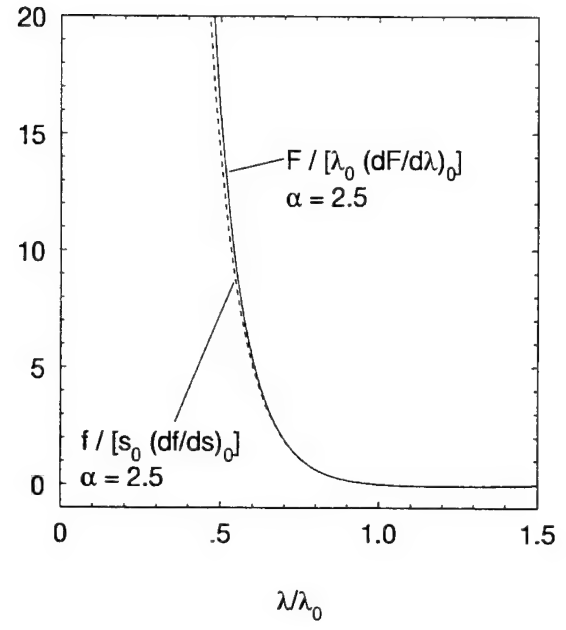

(a)

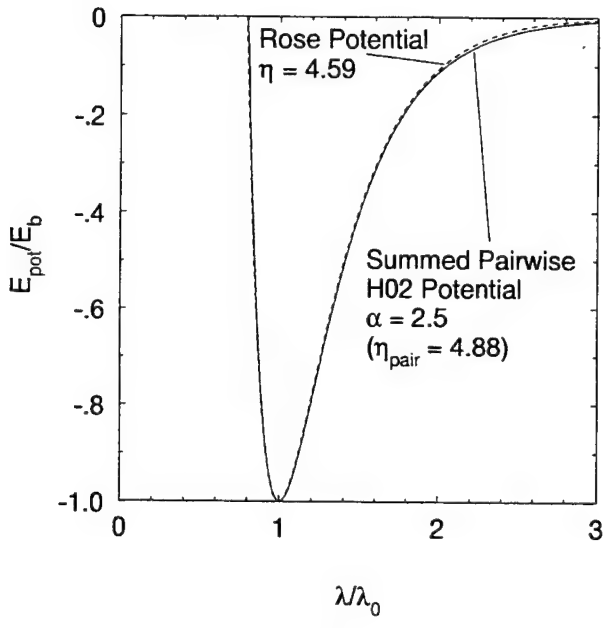

(b)

Figure 1. The pairwise and lattice behavior of an FCC lattice with a pairwise interaction decay rate of $\alpha = 2.5$: (a) nondimensional force; (b) energy potential, depicting differing values for pairwise- and lattice-stiffness, η.

(3) The effective nondimensional stiffness of the lattice, η, is different from, and less than, the stiffness associated with the pairwise interaction, η_{pair}. Though the lattice behavior is nominally describable by the same H02 function as the pairwise behavior, the one notable difference observed at equilibrium between the pairwise and lattice interaction is that the value of the lattice stiffness, $\lambda_0(dF/d\lambda)_0$ differs from the pairwise stiffness, $s_0(df/ds)_0$. One good nondimensional way to express this difference is by way of the η parameter employed by Rose *et al.* [11]. For the pairwise interaction, it is given by

$$\eta_{\text{pair}}^2 = -(df/ds)_0 \, s_0^2 / \varepsilon_b \quad , \tag{8–2}$$

where ε_b is the binding energy of the pairwise interaction. For the full lattice, the nondimensional stiffness is given by

$$\eta^2 = -3 \, (dF/d\lambda)_0 \, \lambda_0^2 / E_b \quad . \tag{8–3}$$

In eqn (8–3), E_b is the binding energy of the lattice. The factor of 3 reflects the definition of lattice force, as introduced in eqn (4–4). Both the pairwise and lattice binding energies are obtainable, from the integration of eqn (8–1) in the case of the pairwise interaction, and from the triple summation of eqn (4–2) for the lattice. In both cases, the minimum in the energy potential is the binding energy. Table 2 shows the comparison of nondimensional stiffnesses (pairwise and lattice) arising from a given interaction decay rate in the H02 potential. As α is lowered, the fact that the nondimensional stiffness of the lattice decreases relative to the pairwise stiffness is indicative of the fact that, for low values of α, the far-field atoms account for an ever-increasing percentage of the lattice's binding energy.

As one of their primary contributions, Rose *et al.* [11] did note the functional similarity between the energy potentials of a great variety of bonding configurations, including metallic as well as diatomic. And though the pairwise bond in a crystal lattice configuration is not identical to the corresponding homopolar bond (because of differing electronic structures), it is not wholly unexpected to find that the (summed) lattice potential does, indeed, follow a form similar to the pairwise potential. Figure 1b depicts the lattice potential for an FCC structure, derived via the

triple summation of eqn (4–2), using a pairwise decay rate of $\alpha = 2.5$, corresponding to $\eta_{pair} = 4.82$ (see Table 2). Closely tracking that curve, shown on the same figure, is the (unsummed) potential of Rose *et al.* [11], employing a value of η equal to 4.55.

Table 2. Nondimensional Stiffnesses[a] as a Function of Interaction Decay Constant

α	η_{pair}	η (η/η_{pair})		
		SC	BCC	FCC
1.1	3.21	2.65 (0.83)	2.65 (0.82)	2.65 (0.82)
1.5	3.70	3.26 (0.88)	3.25 (0.88)	3.25 (0.88)
2	4.26	3.94 (0.92)	3.92 (0.92)	3.92 (0.92)
2.5	4.82	4.56 (0.95)	4.55 (0.94)	4.55 (0.94)
3	5.42	5.15 (0.95)	5.14 (0.95)	5.14 (0.95)
4	6.46	6.27 (0.97)	6.28 (0.97)	6.28 (0.97)
5	7.45	7.34 (0.98)	7.37 (0.99)	7.37 (0.99)

[a] The pairwise and lattice nondimensional stiffnesses were acquired using eqns (8–2) and (8–3), respectively.

One point of note regarding eqn (8–3) is that the parameter η is defined in terms of the slope of the lattice force at the λ_0 lattice-equilibrium reference state. This parameter is a nondimensional measure, therefore, of the lattice stiffness. Nonetheless, Rose *et al.* [11] referred to the parameter η as a measure of the lattice anharmonicity. Though they are technically correct, as shall be shown, we prefer here instead to refer to η as a nondimensional stiffness because of its definition in eqn (8–3).

By contrast, the term anharmonicity characterizes, by definition, the curvature (and not the slope) of the lattice force function because of the fact that the force-curvature for a harmonic spring is identically zero. If we understand the Grüneisen function, Γ, defined in eqn (1–1), to be a measure of the vibrational anharmonicity of the lattice, then we can characterize the volumetric anharmonicity, call it Γ_{vol}, in terms of a definition similar to eqn (1–1). Relating ω

back to the vibrational stiffness by way of eqn (2–2) and expressing the volume-derivative in terms of λ instead, eqn (1–1) may be expressed as

$$\lambda^3/\psi = \Gamma = -(\lambda/6)\,[d/d\lambda(\partial F_{vib}/\partial x)] \;/\; (\partial F_{vib}/\partial x) \quad . \tag{8–4}$$

A corresponding definition for volumetric anharmonicity, employing the volumetric rather than the vibrational stiffness, would follow as

$$\Gamma_{vol} = -(\lambda/6)\,(d^2F/d\lambda^2) \;/\; (dF/d\lambda) \quad . \tag{8–5}$$

Were one to convert λ back into V, and substitute $F = p_c\lambda^2 = p_c V^{2/3}$, eqn (8–5) could be shown to be precisely the relationship derived by Dugdale and MacDonald [5] for Γ, who had assumed (along with many others) that the volumetric and vibrational stiffnesses were functionally identical. Table 3 provides a comparison of these two metrics under various conditions. Note, however, that Γ in the present study is composed only of the longitudinal and transverse stiffnesses along the principal directions of the lattice, whereas a full accounting of Γ would include the effects from all lattice modes. We know from the work of Dugdale and MacDonald [5], for example, that measured values for vibrational- and volumetric-Γ_0, for real materials, are generally closer to each other than is reflected in Table 3. However, though the value for Γ_0 may be incorrect as a result of accounting for the vibrational modes only along the principal direction of the lattice, it may still be reasonable to assume that the manner in which these modes functionally change with lattice spacing is characteristic of how the other modes change.

If an energy potential, one that precisely satisfied Rose's energy potential, were evaluated in eqn (8–5) at the reference λ_0 state, the derived value of Γ_{vol0} would be $\eta/2.6$ (or $2.3\eta/6$, to be precise). We therefore see why Rose *et al.* referred to η as an anharmonicity parameter, even though its actual definition, eqn (8–3), characterizes a nondimensional stiffness: because of the particular form of their energy potential, the parameter η (or more accurately $\eta/2.6$) characterizes the volumetric anharmonicity, as well.

Table 3. Equilibrium Values for the Vibrational[a] and Volumetric Γ

α	Γ_0 (Γ_{vol0})		
	SC[b]	BCC	FCC
1.1	0.72 (1.37)	0.70 (1.37)	0.70 (1.36)
1.5	0.89 (1.49)	0.83 (1.48)	0.83 (1.48)
2	1.10 (1.65)	1.01 (1.64)	1.00 (1.64)
2.5	1.31 (1.82)	1.19 (1.81)	1.17 (1.81)
3	1.52 (1.98)	1.38 (1.97)	1.36 (1.97)
4	1.92 (2.32)	1.74 (2.31)	1.72 (2.31)
5	2.32 (2.65)	2.09 (2.65)	2.09 (2.65)

[a] Vibrational Γ computed from principal stiffnesses only.
[b] Vibrational Γ for simple cubic lattice computed from longitudinal stiffness only, as SC lattice not stable in shear, along the principal lattice directions.

Even though the triple-summed energy potential in the current effort, eqn (4–2), is nominally describable by Rose's potential (Figure 1b), it would be presumptious to conclude that Γ_{vol0} will always equal $\eta/2.6$. Therefore, we should use Γ_{vol0} rather than η to characterize the volumetric anharmonicity. For the case of pairwise interactions only, where the H02 potential has been assumed as the governing form, the relation $\Gamma_{vol0} = 1 + \alpha/3$ governs the pairwise curvature at the equilibrium state.

The volumetric anharmonicity, Γ_{vol0}, since it defines the curvature of the lattice force at the λ_0 state, should also be relatable to the parameter B', which is employed by a number of authors [15–19], and represents the pressure derivative of the bulk modulus, B, as

$$B' = (\partial B/\partial p)_T \quad , \tag{8–6}$$

though some authors have defined this derivative as being at constant pressure, not temperature. The confusion arises because eqn (8–6) defines a curvature along the reference isotherm.

However, actual data tend to be obtained from a number of data points at constant pressure. The expression B'_0 refers to this quantity at the reference state of zero temperature and pressure. If we expand the definition of B as $-V(\partial p/\partial V)_T$, then eqn (8–6) may be expressed as

$$B' = -1 - V(\partial^2 p/\partial V^2)_T / (\partial p/\partial V)_T \quad . \tag{8–7}$$

Eqn (8–7) looks very similar to the definition of Γ proposed by Slater [2], Γ_{Sl}, and may be related to it as

$$\Gamma_{Sl} = -1/6 + B'/2 \quad . \tag{8–8}$$

A relation similar to this was actually posited by Syassen and Holzapfel [18], though their relation was based on model calculations, and not derived. At the reference state only, the value for Γ_0 predicted by Slater's model is 1/3 in excess of the value later predicted by Dugdale and MacDonald's model [5], $\Gamma_{DM0} = \Gamma_{Sl0} - 1/3$. And since eqn (8–5) indicated that the Dugdale-MacDonald Γ_{DM} was, in fact, Γ_{vol}, we therefore have that

$$\Gamma_{vol0} = -1/2 + B'_0/2 \quad . \tag{8–9}$$

This equation constitutes yet one more method for estimating Γ_{vol0}, though there appears to be wide scatter in the experimental measurement of B'_0, more so than in the estimation of η.

(4) The vibrational and volumetric spring constants are quantitatively distinct functions. Perhaps a primary result of this analysis is quantitatively verifying the distinct nature of the volumetric and vibrational stiffness of an atomic lattice, a distinction which has been recently asserted on qualitative grounds [13] but one which contradicts the assumption employed by many previous analyses on the subject [2, 5, 6–9]. Since the distinction is shown to arise from the influence of nonnearest neighbors, we might expect the magnitude of the discrepancy to be greater for low-decay-rate interactions. Figures 2 and 3 bear this hypothesis out by depicting a comparison of the volumetric and vibrational stiffnesses for two FCC lattices of differing stiffnesses. In terms of absolute, not relative, quantities, Figure 4 displays the energy, force, and stiffnesses of an FCC, $\alpha = 5$ lattice.

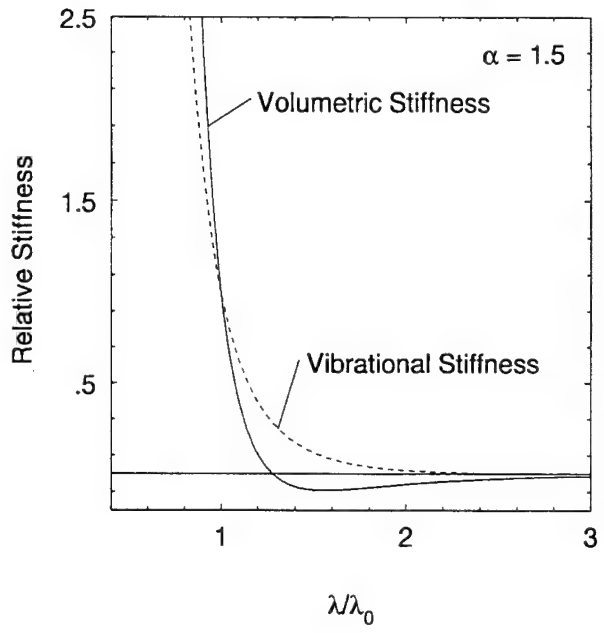

(a)

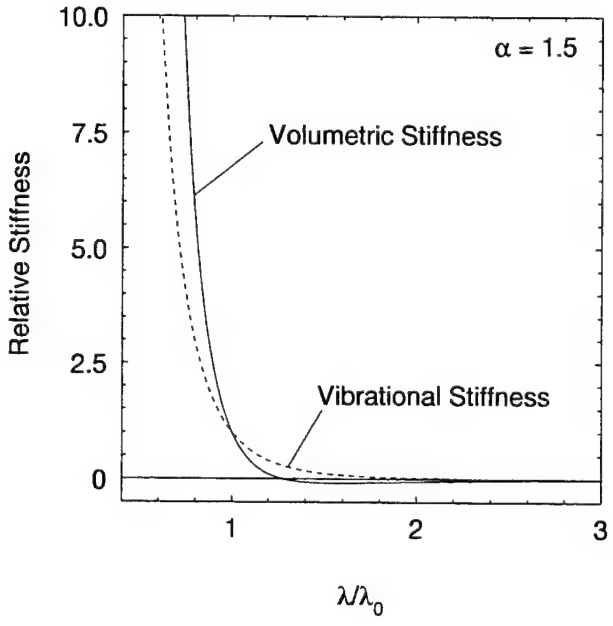

(b)

Figure 2. A relative comparison of the volumetric stiffness, $dF/d\lambda$, to the vibrational stiffness, $\partial F_{vib}/\partial x$, for an FCC lattice with a pairwise, interaction decay rate of $\alpha = 1.5$: (a) to 2.5 times the nominal stiffness; (b) to 10 times the nominal stiffness.

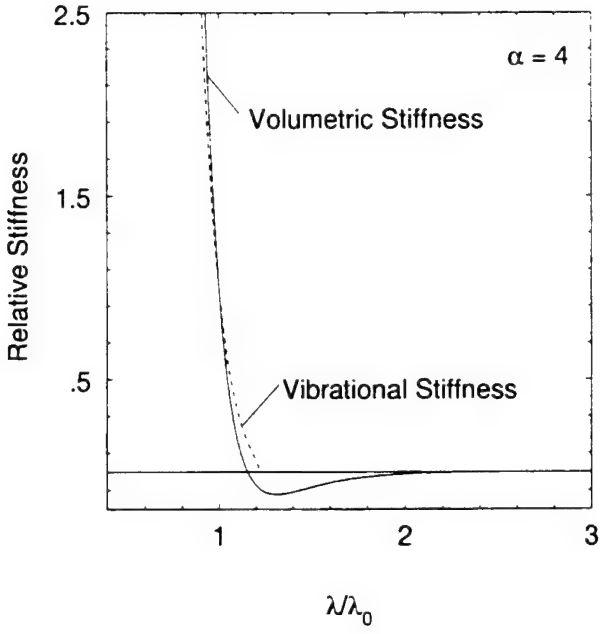

Figure 3. A relative comparison of the volumetric stiffness, $dF/d\lambda$, to the vibrational stiffness, $\partial F_{vib}/\partial x$, for an FCC lattice with a pairwise, interaction decay rate of $\alpha = 4$.

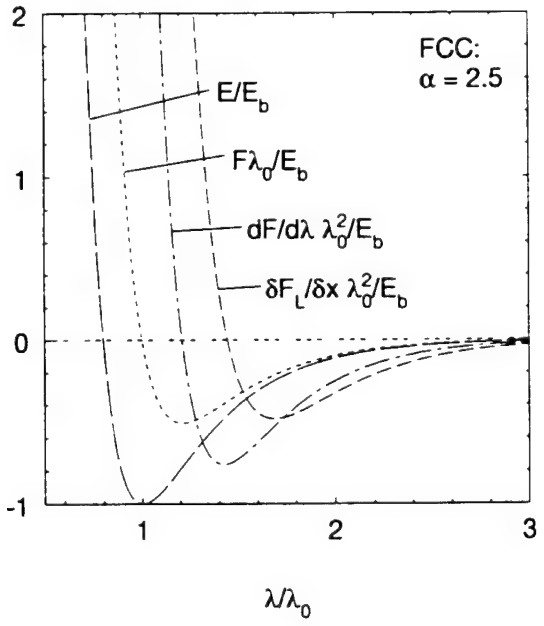

Figure 4. The energy, force, and volumetric and vibrational stiffnesses for an FCC $\alpha = 2.5$ lattice, shown in comparison to each other (note that the stiffness functions are shown as positive in compression for convenience in visualization).

(5) The zero of the vibrational spring constant is observed to be at a value of λ greater than the zero of the volumetric spring constant. As α decreases, the distance between these zeroes increases as well. For low values of pairwise stiffness, the zero of the vibrational stiffness can be significantly different from that of the volumetric stiffness. For the $\alpha = 1.5$ case depicted in Figure 2, the zeroes of the volumetric and vibrational stiffness occur at λ/λ_0 values of 1.28 and 2.41, respectively. This difference in lattice spacing corresponds to a huge difference in relative volumes, V/V_0, of 2.1 and 14.0, respectively. At a large enough expansion, however, even the vibrational stiffness is observed to become negative. When the vibrational stiffness becomes negative, the characteristic frequency, ω, becomes undefined and the Grüneisen relationship, eqn (1–1), breaks down. The zero of the volumetric spring constant (*i.e.*, the inflection point of the energy potential) has been associated with a metal's melting point [9], and perhaps it is this phase change to a liquid, not considered in this study, that in reality precludes the Grüneisen singularity associated with the zero of the vibrational spring constant.

(6) The value of the Grüneisen function, Γ, is observed to approach 2/3 in the high-compression limit. By contrast, Γ_{vol} does not. Eqn (8–4) shows how the Grüneisen function (and $\psi = V/\Gamma$) may be evaluated when the vibrational stiffness is known. The stiffness itself is obtained from eqn (7–2) and its derivative with respect to λ from eqn (7–3). Alternately, longitudinal- and transverse-component values of Γ may be obtained by using the L and/or T component values directly in eqn (8–4). The value for ψ at any given value of λ is V/Γ, alternately λ^3/Γ. A typical example of the Γ function, as computed in this manner, is shown in Figure 5 (expressed in λ, not V), along with ψ. For illustration, both the L and T component contributions are shown as well.

The functional form for ψ has been observed to be similar in appearance (to that of Figure 5) over the full range of cases tested. Therefore, we seek to further examine the nature of this function. The H02 potential, as noted by the authors [15], exhibits the proper functional form in the high-compression limit. We would, therefore, hope that the evaluation of ψ and Γ by way of eqn (8–4) would do the same. In fact, we note here that, regardless of the value employed for α, or the lattice structure employed, the limiting high-compression value for Γ approaches the recognizable value of 2/3. By contrast, were there no distinction made between

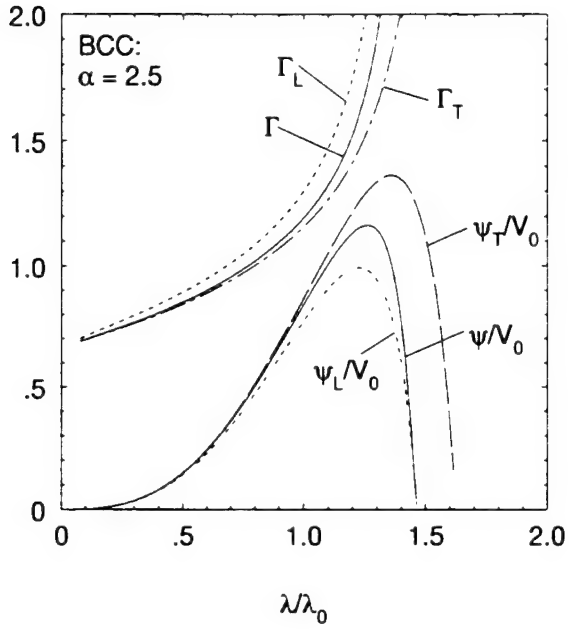

Figure 5. The Γ and corresponding ψ functions for an $\alpha = 2.5$, BCC lattice, showing both the *L* and *T* components, as well as the aggregated function.

the vibrational and volumetric stiffness, then Γ_{vol}, evaluated by way of eqn (8–5), should instead provide the proper limiting behavior of 2/3. However, Γ_{vol} has been observed *not* to approach this limiting value. The only way that Γ_{vol} could approach the proper limiting value, given the H02 pairwise potential, would be if interactions beyond the nearest neighbors were ignored. Unfortunately, no matter how large an interaction decay constant, α, might be chosen in an attempt to eliminate the influence of all but the nearest of neighbors, the nearest nonneighbors will nonetheless have an effect in the high-compression limit, since no matter how much α is increased, λ may shrink toward zero a corresponding amount in order to achieve the same relative influence of its nonnearest neighbors.

Considering the other end of the domain, at large λ, a negative slope on ψ has been associated with one type of thermodynamic instability at elevated temperatures [20]. We, therefore, examine the state of the lattice interactions at this critical point where $d\psi/dV = 0$. If we denote, at this maximum in the ψ curve, the lattice spacing as λ_{stab} and the distance to an atom's nearest neighbor in the lattice as s_{stab}, then we may learn something by the behavior of these variables as a function of pairwise stiffness and lattice structure. Table 4 portrays these variables in a normalized form. The results show behavior that is somewhat uniform across lattice structures (allowing for the fact that the SC lattice calculations are based on longitudinal stiffness only). Examining s_{stab}, the values relative to s_0 are, in addition, nearly independent of the interaction decay rate, α. One may conclude from this, regardless of lattice structure and stiffness, that the extremum in the ψ curve occurs when the interatomic distance to the nearest neighbor in the lattice is approximately equal to the equilibrium spacing associated with the pairwise potential. At such a lattice spacing, this nearest neighbor is barely applying any force at all, and all neighbors beyond s_0 are applying an attractive force. Thus, the maximum of the ψ function occurs, for a variety of lattice structures and over a large range of nondimensional stiffness, at nearly the identical relative pairwise configuration—a configuration associated with a minimal pairwise interaction from the nearest neighbor.

Considering, however, the situation in terms of the lattice behavior, as opposed to the pairwise interactions, an examination of λ_{stab} values from Table 4 reveals where the equilibrium spacing for the lattice falls relative to the critical spacing. At low decay-rate values, the critical

value for λ falls at several times the equilibrium spacing for the lattice. As the decay rate is increased, however, Table 4 reveals that the equilibrium lattice spacing approaches the critical value for λ.

Table 4. Critical Lattice Spacings Associated with $d\psi/dV = 0$[a]

α	λ_{stab}/λ_0 (s_{stab}/s_0)		
	SC[b]	BCC	FCC
1.1	7.09 (0.90)	7.34 (1.00)	7.39 (1.03)
1.5	2.04 (0.92)	2.10 (1.00)	2.12 (1.04)
2	1.42 (0.93)	1.46 (1.00)	1.48 (1.04)
2.5	1.22 (0.93)	1.26 (1.00)	1.27 (1.04)
3	1.13 (0.93)	1.16 (1.00)	1.17 (1.03)
4	1.04 (0.93)	1.07 (0.98)	1.07 (1.01)
5	1.00 (0.93)	1.02 (0.97)	1.02 (1.00)

[a] The ψ function computed from principal stiffnesses only.
[b] The ψ function for simple cubic lattice computed from longitudinal stiffness only, as SC lattice is not stable in shear, along the principal lattice directions.

PART II—Macroscopic Lattice Behavior

9. Mechanical Characteristics of the Lattice

The summed lattice equations that have been derived in Part I [eqns (4–2), (4–7), (4–8), (7–2) and (7–3)] depict a methodology for modeling the interatomic forces and vibrational characteristics of an atomic lattice. As a paradigm, it is simple, complete, and of general applicability. Unfortunately, from a practical point of view, a triple summation is an inefficent vehicle by which to computationally describe the behavior of a lattice. Furthermore, the insights provided by the triple summation are limited in scope.

It was, therefore, a goal in this study to capture the essence of the governing equations, which involve triple summations, in terms of a simpler analytical formulation. Our approach is to examine separately the mechanical and the thermal characteristics of the summed lattice equations, each in terms of the lattice's vibrational behavior. These separate mechanical and thermal models can then be combined into a unified equation of state.

Based in part on the semi-empirical form of eqn (2–1), similar looking forms were tested in an attempt to analytically describe the summed lattice force without the use of fitting parameters. A remarkably good fit was found possible, over a wide range of stiffnesses and lattice spacings, with the following form:

$$\frac{F}{-\lambda_0 (dF/d\lambda)_0} = \frac{1}{3\Gamma_0 (\lambda/\lambda_0)^2} (\omega/\omega_0)^{\beta} \ln(\omega/\omega_0) \quad . \tag{9–1}$$

This form is guaranteed to provide slope compatibility of the force at λ_0, while the parameter β is selected to guarantee curvature compatibility in the lattice force at λ_0. That requirement dictates that

$$\beta = [\Gamma_{vol0} - 1/3 - 1/2 \cdot \Gamma_0 (d\psi/dV)_0] / \Gamma_0 \quad , \tag{9–2}$$

Furthermore, we note that β is obtainable from material properties at the force-free equilibrium state.

Let us recall that given in this problem is a known pairwise interaction potential, integrated from eqn (8–1), which is characterized by the parameters α, s_0, and $s_0(df/ds)_0$. Through direct differentiation of this pairwise force, the pairwise stiffness may be readily obtained. In eqn (9–1), which we propose to employ to characterize the behavior of the full lattice, λ_0 and $\lambda_0(dF/d\lambda)_0$ are computed from the equilibrium condition of eqn (4–2). The parameter β may be computed from eqn (9–2). The ratio (ω/ω_0), from the definition in eqn (2–2), is given as

$$\omega/\omega_0 = [\partial F_{vib}/\partial x \; / \; (\partial F_{vib}/\partial x)_0 \,]^{1/2} \quad . \tag{9–3}$$

Both of the constituent terms composing the right-hand side of eqn (9–3) are obtained by way of eqn (7–2). The value for Γ_0 may be obtained from eqn (8–4), being evaluated at the equilibrium value of lattice spacing.

Thus, we are able to evaluate eqn (9–1) without the use of fitting parameters and compare the result to the force, F, obtained by way of the triple summation of eqn (4–7). Figure 6 shows examples of the quality with which eqn (9–1) may describe the lattice force over a wide range of interatomic decay rates. The fits are for an FCC crystal, though the other crystal types (*e.g.*, SC and BCC) show identical trends with comparable accuracy. The comparisons are shown to a compression corresponding to a stiffness of 15× the equilibrium stiffness, which, in all cases shown, corresponds to a maximum relative-volumetric compression at or beyond $V/V_0 = 0.22$ (λ/λ_0 at or beyond 0.6). The comparison is of excellent quality for the low- and mid-range decay rates, though it does begin to deviate somewhat for the $\alpha = 5$ case.

It should be noted that, unlike eqn (4–7), which is valid for all λ states, the analytical, frequency-based eqn (9–1) can only apply where a vibrational frequency, ω, is definable. When $\partial F_{vib}/\partial x$ changes sign (at some expansion beyond the inflection point in the lattice potential,

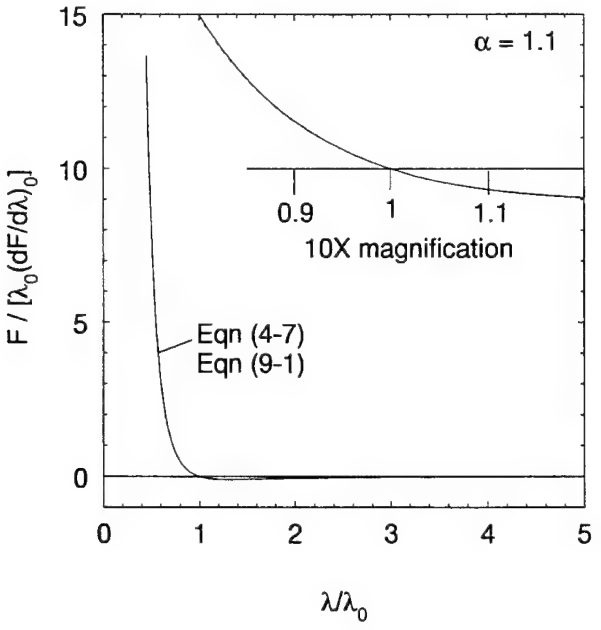

(a)

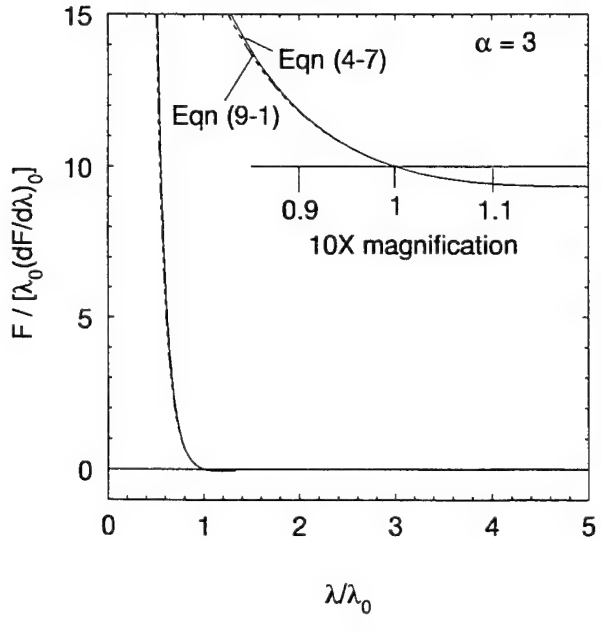

(b)

Figure 6. A comparison of the numerically computed (summed) lattice force [eqn (4–7), solid line] to that analytically evaluated by way of eqn (9–1) (dashed line), for an FCC lattice of: (a) $\alpha = 1.1$; (b) $\alpha = 3$; (c) $\alpha = 5$.

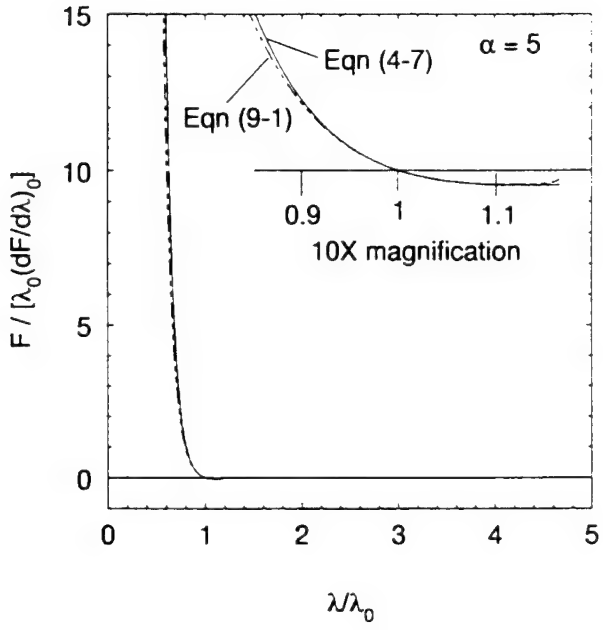

(c)

Figure 6. A comparison of the numerically computed (summed) lattice force [eqn (4–7), solid line] to that analytically evaluated by way of eqn (9–1) (dashed line), for an FCC lattice of: (a) $\alpha = 1.1$; (b) $\alpha = 3$; (c) $\alpha = 5$.

eqn (9–1) can no longer apply. Of course, by this level of expansion, $dF/d\lambda$ has already changed sign, whereupon the lattice can no longer remain mechanically stable (*i.e.*, any slight deviation from the ideally spaced lattice configuration will result in negative restoring forces, which will effectively tear apart the lattice).

10. Thermal Characteristics of the Lattice

Whereas the interatomic potential is responsible for the lattice's zero-temperature, force of repulsion, as computed by eqn (4–7), thermal excitations also add to the net interatomic repulsion. Though temperature is a direct measure of the thermal excitations, the internal energy of thermal excitation, $E_{th} = (E - E_{pot})_V$, is directly related to the temperature by way of the specific heat function and is, therefore, another measure of the thermal excitation. As noted in this paper's introduction, it is the Grüneisen function, Γ, that directly relates a material's thermal energy change to a change in pressure. Knowledge, therefore, of the Γ (or, alternately, ψ) function, in addition to the lattice potential, constitutes a complete, thermal equation of state. Note, however, that because the vibrational stiffness modeled in this paper is not considered to be a function of vibrational amplitude [*i.e.*, infinitesimal amplitudes have been assumed as part of eqn (2–2)], the current analysis will necessarily compute Γ as a function of volume only. Fortunately, such an assumption is widely accepted in the community, over a large range of temperatures.

In addition to being analytically related to ω by way of eqn (1–1), it was noted that the ψ function could be fit to ω in another manner, again over a wide range of lattice spacings and interaction decay rates. The form of the fit is given by

$$\psi/\lambda^4 = \psi/V^{4/3} \sim \omega^{\xi} \quad , \tag{10–1}$$

where ξ is a parameter that can be fitted for a given lattice configuration and decay rate. Figure 7 provides an example of the quality of this correlation. Similarly good correlations were noted for other lattice types and decay rates, with values for ξ approaching 0.50 for low

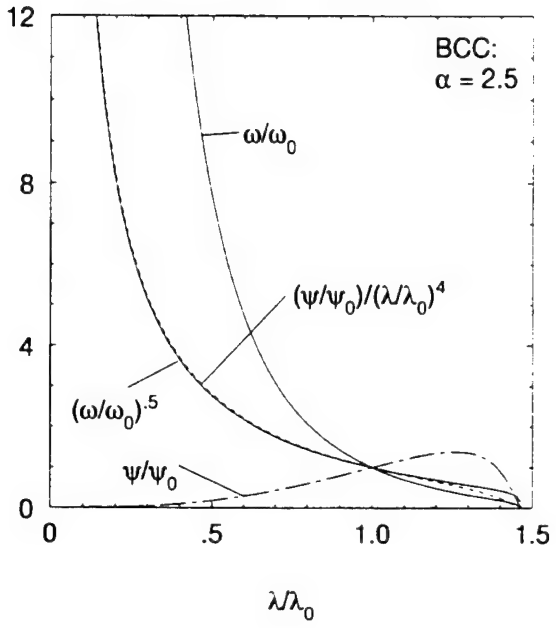

Figure 7. The functional correlation of the (ψ/λ^4) function to ω^{ξ}, for an $\alpha = 2.5$, BCC lattice.

stiffnesses ($\alpha \sim 1.1$) and rising to approximately 0.56 for high stiffnesses, regardless of lattice structure ($\alpha \sim 5$).

Though we know of no theoretical reason why the correlation described by eqn (10–1) should hold true, a further measure of the quality of the correlation may be obtained by differentiating eqn (10–1) with respect to V and dividing the result by eqn (10–1) itself. Substitution of eqn (1–1) into the result allows for the elimination of ω, to obtain

$$\xi = 4/3 \cdot \psi/V - d\psi/dV \quad . \tag{10–2}$$

Effectively, eqn (10–2) compares not the values of the terms composing eqn (10–1), but rather their derivatives, and is thus a more stringent comparison of the correlation. Figure 8 depicts, for the same lattice configuration employed in Figure 7, the two terms on the right-hand side of eqn (10–2). Based on the fitting form, the vertical distance between the two curves should be a constant, and is a measure of ξ. The correlation is seen to hold over the compressive domain and only begins to diverge at the larger lattice spacings, near and beyond the critical value of λ, where $d\psi/d\lambda$ changes sign.

Furthermore, by evaluating ψ and its derivative at the equilibrium lattice spacing, λ_0, eqn (10–2) provides a nonempirical way to select a value for ξ. Of course, evaluating ξ in this manner does not necessarily provide the best-fit for ψ over a wide range of λ—however, it does guarantee that the analytical function represented by eqn (10–2) will match the value and slope of ψ at λ_0, otherwise obtained from the triple-summation method. Whereas a good fit to eqn (10–1) over a wide range of λ was obtained in Figure 7 with a value of $\xi = 0.50$, the use of eqn (10–2) to analytically evaluate ξ at the λ_0 reference condition provides a slightly altered value of $\xi = 0.538$, which we use for the remainder of this comparison.

A solution to the differential equation, eqn (10–2), is

$$\psi/V_0 = 3\xi\,(V/V_0) - (3\xi - 1/\Gamma_0)\,(V/V_0)^{4/3} \quad . \tag{10–3}$$

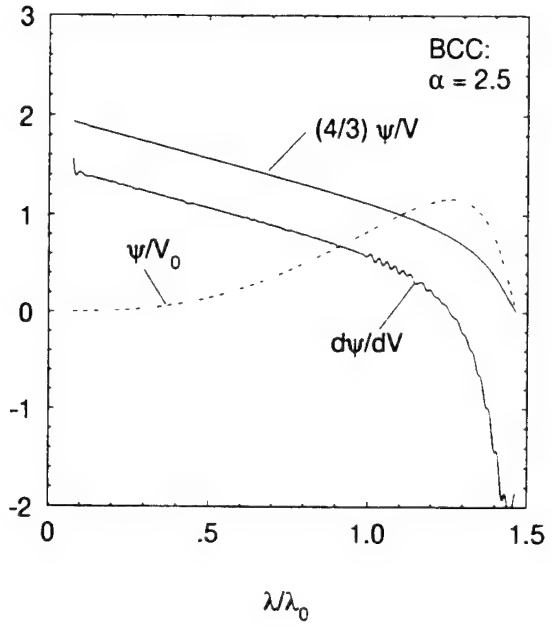

Figure 8. Comparison of 4/3 $\cdot \psi/V$ and $d\psi/dV$ for an $\alpha = 2.5$ BCC lattice. Note that $d\psi/dV$ equals $(d\psi/d\lambda)/(3\lambda^2)$.

When we compare this explicit form for ψ to that computed from the pairwise summation by way of eqns (7–2), (7–3), and (8–4), we find, in Figure 9a, a good match into the compressive regime, with a divergence noted in the expanded states of the lattice, near and beyond the maximum in ψ. If we invert ψ from Figure 9a and express the result in terms of Γ, as in Figure 9b, we see that at high compressions, results may deviate as well. The reason here is clear: in order that $\Gamma_{\lambda \to 0} = 2/3$, ξ must necessarily take on a value of 1/2. As noted previously, values for ξ required to fit eqn (10–1) fall in the 0.5 to 0.56 range. What this says is that eqn (10–1) is, at best, a fit but that the range of lattice spacing over which this fit applies can be quite large, indeed. Recall, as well, that $V/V_0 = (\lambda/\lambda_0)^3$, and so divergence of the fit at a relatively small value of λ corresponds to an extremely compressed state in terms of V.

Eqn (1–1) may be integrated, in light of eqn (10–3), to recover a functional form for the lattice frequency. Again, like eqns (10–2) and (10–3), this computed frequency is based upon the correlation cited in eqn (10–1). The result is

$$\omega/\omega_0 = [3\Gamma_0 \xi (\lambda_0/\lambda - 1) + 1]^{1/\xi} \quad . \tag{10–4}$$

Figure 9c shows the analytically computed frequency of eqn (10–4) compared to the summed value for ω/ω_0, acquired from eqn (9–3) by way of the triple summation of eqn (7–2). To more fully ascertain the effect of the divergence noted in Figures 8 and 9a, we zoom in on the low-frequency, expanded lattice region of Figure 9c and present the result as Figure 9d.

Even though the parameter ξ may be obtained from known material properties at the λ_0 reference state, the fact remains that eqn (10–3) is still a simplified fit to the actual functional form exhibited by the ψ variable. At large compressions, the form of eqn (10–3) may diverge from data. At large expansions, as well, there is a rather notable departure of eqn (10–3) from the actual value for ψ. Because values for λ_{stab}/λ_0, as given in Table 4, are large for small α, the analytical equations deriving from the fit to eqn (10–1) should be accurate at the nominal lattice spacing and to quite an extent into the expanded regime for small α. By contrast, for large values of α, the analytical fit associated with eqn (10–3) will be valid over a much smaller range of expanded states because the λ_0 reference state is at the point of greatest curvature in the

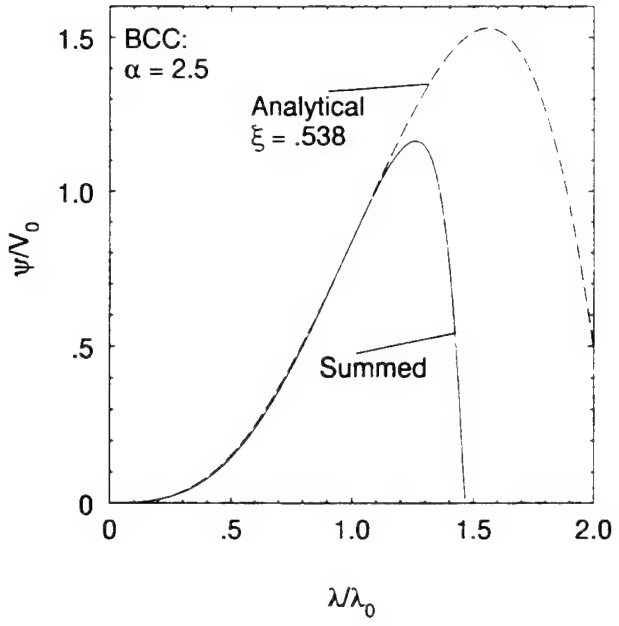

(a)

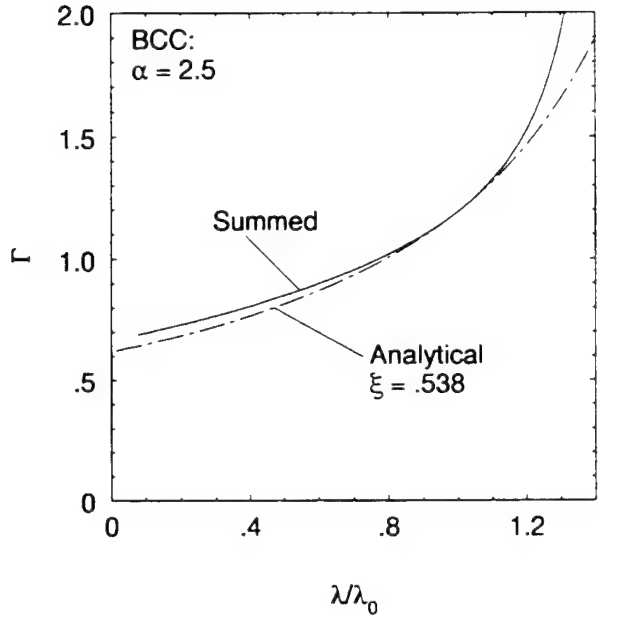

(b)

Figure 9. A comparison of the computed (summed) lattice properties to the analytical fit implied by eqns (10–3) and (10–4) for an $\alpha = 2.5$, BCC lattice: (a) ψ/V_0; (b) Γ; (c) ω/ω_0 (compression); and (d) ω/ω_0 (expansion).

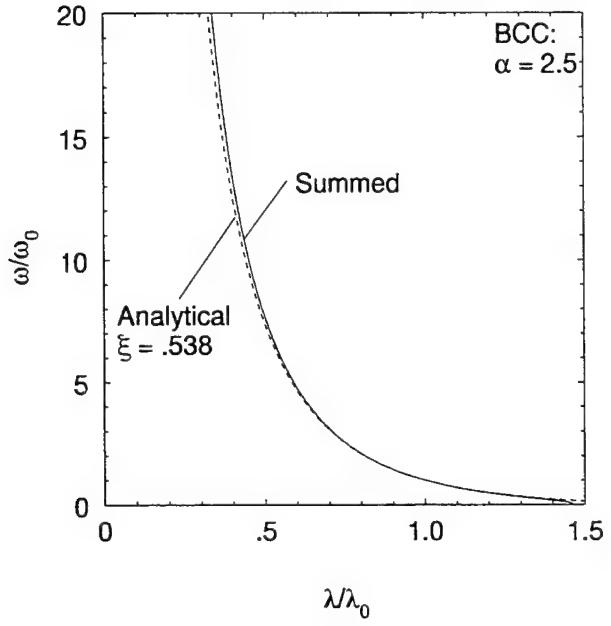

(c)

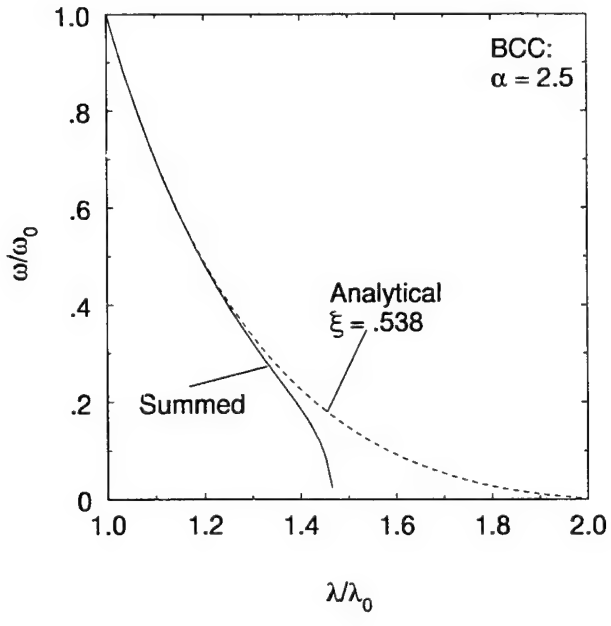

(d)

Figure 9. A comparison of the computed (summed) lattice properties to the analytical fit implied by eqns (10–3) and (10–4) for an $\alpha = 2.5$, BCC lattice: (a) ψ/V_0; (b) Γ; (c) ω/ω_0 (compression); and (d) ω/ω_0 (expansion).

$\psi(\lambda)$ curve. Clearly, the eventual solution to this dilemma is a better-fitting functional form for ψ, in preference to eqn (10–3). Nonetheless, the simplicity offered by eqn (10–1) and the equations derived from it will help us to formulate, in the next section, a complete, thermal equation of state, capable of modeling general thermodynamic transitions and not only zero-temperature ones.

Interestingly, in the low-α limit, where ξ approaches 1/2 and Γ_0 (see Table 3) approaches 2/3, we have from eqns (10–3) and (10–4) that $\psi = 3/2 \cdot V$ and $\omega \sim \lambda^{-2}$. The conclusions, in this limiting case only, are that: Γ is a constant, equal to 2/3; λ_{stab} approaches infinity; and the vibrational stiffness never changes sign, such that ω is defined out to infinite lattice separation.

11. A Frequency-Based Analytical Equation of State

The lattice force description, given by eqn (9–1), has been shown to describe the behavior of SC, BCC, and FCC lattices over a wide range of lattice spacings and interatomic, interaction-decay rates, α. When given a pairwise potential, no fitting parameters are required in order to describe the mechanical behavior of the lattice. By contrast, the semi-empirical equation-of-state form given by eqn (2–1), similar in form to eqn (9–1), requires one fitting parameter to describe the functional behavior of ψ, since there is no pairwise potential from which eqn (2–1) derives. The semi-empirical form, eqn (2–1), does, however, have one advantage over eqn (9–1)—that it may be readily integrated, because of the ψ term, to yield the lattice potential as

$$E_{pot} = -E_b \, (\omega/\omega_0)^K \, [1 - \ln(\omega/\omega_0)^K] \quad , \qquad (11\text{–}1)$$

whereas eqn (9–1) cannot be integrated without first specifying the manner in which ω is coupled to λ.

However, begining with the lattice force given by eqn (9–1) and substituting the observed correlation given by eqn (10–1) into it [in effect, multiplying by unity in the form of $(\omega/\omega_0)^{\xi} \cdot (\lambda/\lambda_0)^4 / (\psi/\psi_0)$], one may obtain

$$\frac{F}{-\lambda_0 (dF/d\lambda)_0} = \lambda_0/(3\Gamma_0^2) \cdot \lambda^2/\psi \cdot (\omega/\omega_0)^{(\xi+\beta)} \ln(\omega/\omega_0) \quad . \tag{11–2}$$

In deriving eqn (11–2), use has been made of the definition, given in (1–1), that $\psi = V/\Gamma$. A comparison of this result to eqn (2–1) reveals identical forms with but one exception—in the semi-empirical form, the exponent on the lattice frequency term is K, whereas in the present analysis, it is $(\xi + \beta)$. Based on the the values of ξ and β determined for the lattices studied, one would expect to find values for the exponent roughly in the 4/3 to 5/3 range. By contrast, values for K display a range of 2/3 to 4/3.

The reason that the semi-empirical eqn (2–1) retained K as the exponent on ω arose from the mistaken belief that ω remained definable out to infinite expansions and that the form of the potential, eqn (11–1), should continue to fit the data as $\lambda \rightarrow \infty$. In contrast, the current analysis, leading to the explicit, triple-summation calculation of $\partial F_{vib}/\partial x$ and ω, has shown that at large enough expansions the vibrational stiffness changes sign and, thus, the characteristic lattice frequency becomes undefined beyond that point. Acknowledging, therefore, the inability of any frequency-based equation of state for solids to capture the highly expanded behavior of the lattice potential, the requirement for retaining the exponent on ω equal to the value K is no longer imperative.

Unlike eqn (9–1), eqn (11–2) now becomes directly integrable to acquire the energy potential. If we: (1) denote the sum, $\xi + \beta$, as κ; (2) recall that $F = p_c \lambda^2$; (3) express $-\lambda_0 (dF/d\lambda)_0$ in terms of the equilibrium bulk modulus, B_0, as $-\lambda_0 (dF/d\lambda)_0 = 3B_0 \lambda_0^2$; and (4) reference the energy zero to the equilibrium lattice state, such that $E_c = E_{pot} + E_b$; then the lattice pressure and energy may be expressed as

$$p_c = F/\lambda^2 = B_0 V_0/\Gamma_0^2 \cdot (\omega/\omega_0)^{\kappa} \ln(\omega/\omega_0)/\psi \tag{11–3}$$

$$E_c = B_0 V_0/(\Gamma_0 \kappa)^2 \{1 - (\omega/\omega_0)^{\kappa} [1 - \ln(\omega/\omega_0)^{\kappa}]\} \quad . \tag{11–4}$$

The quantity $B_0 V_0$, appearing only as a product, may be replaced by the square of the equilibrium, bulk sound speed, C_0^2. Note also that, unlike eqn (9–1), the H02 potential, or many of the other popular potentials in use, eqns (11–3) and (11–4) are functions only of the lattice frequency and its derivatives. Lattice spacing, *per se*, has been removed completely as an independent variable!

We may compare the results of eqns (11–3) and (11–4) to the triple-summed force and energy calculations given by eqns (4–5) and (4–2), respectively. We do so in Figure 10 for two cases of α. In compression (Figures 10b and 10d), the analytical result for F is within 2% of the summed result to a relative lattice spacing of 0.584 ($V/V_0 = 0.20$) in the case of $\alpha = 2$, and 0.578 ($V/V_0 = 0.19$) in the case of $\alpha = 5$. In expansion (Figures 10a and 10c), the analytical forms do an excellent job out to $\lambda = \lambda_{stab}$ and rapidly diverge beyond that point. As mentioned earlier, the analytical forms are only defined out to the lattice spacing where ω goes to zero, which is usually rather close in value to λ_{stab}. From this, we may surmise that the analytical form does an excellent job of representing the lattice composed of discrete atoms by way of a continuous function, as long as the granularity of the lattice (spacing normalized by some function of α) is not too large. The parameter λ_{stab} is an approximate measure of this granularity, defining a cutoff point beyond which the analytical result will eventually diverge from the discretized reality of an actual lattice. To show that the analytical equations above are capable of capturing the highly expanded behavior of the lattice, when the granularity is low, we provide Figure 11, depicting the potential and force for an $\alpha = 1.1$ lattice. In this case, the value of λ_{stab}/λ_0 does not occur until a value in excess of 7.3. Thus, for lattice spacings smaller than this amount, as depicted in the figure, the analytical forms (dashed lines) do a good job of matching the summed equations (solid lines).

Even though the fits entailed in eqns (10–1)–(10–4) were employed in the development of eqns (11–3) and (11–4), the results portrayed in Figures 10 and 11 employ the *actual values* for ω and ψ arising from the triple summations and not some fitted form for their behavior. Thus, eqns (11–3) and (11–4) are seen *not* to require an artificially imposed functional behavior for ψ or ω [*i.e.*, the primary purpose of eqn (10–1) was to assist in the development of

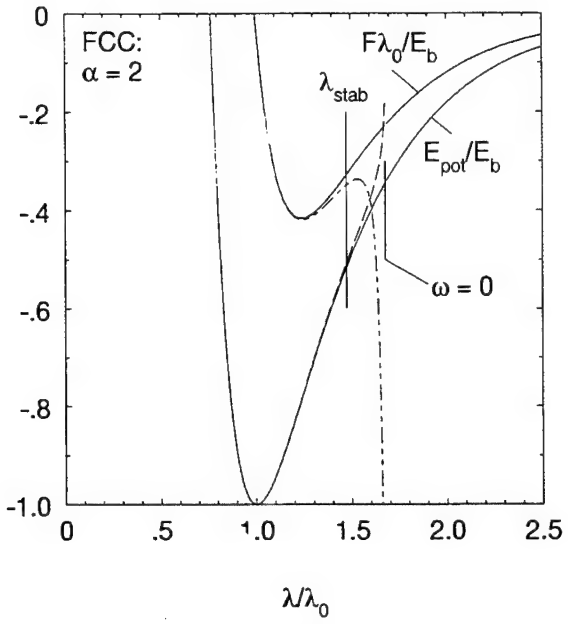

(a)

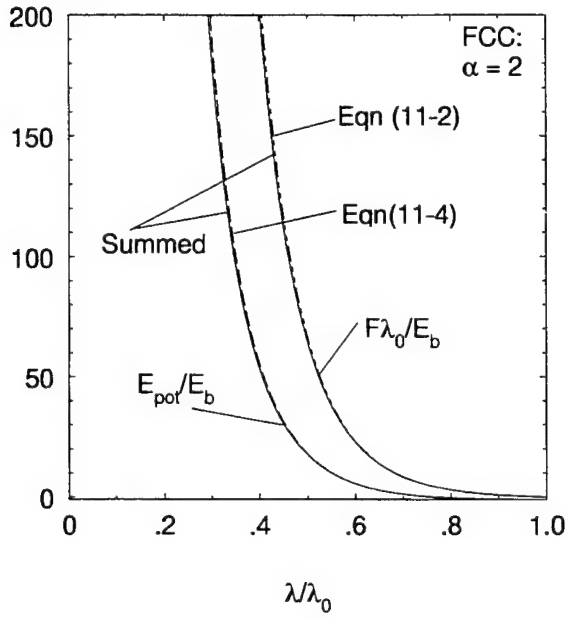

(b)

Figure 10. A comparison of the lattice's energy potential and force (solid lines) to the analytical, frequency-based result (dashed lines): (a) FCC, $\alpha = 2$ (expansion); (b) FCC, $\alpha = 2$ (compression); (c) FCC, $\alpha = 5$ (expansion); (d) FCC, $\alpha = 5$ (compression). Shown on (a) and (c) are lattice spacings corresponding to λ_{stab} and $\omega = 0$.

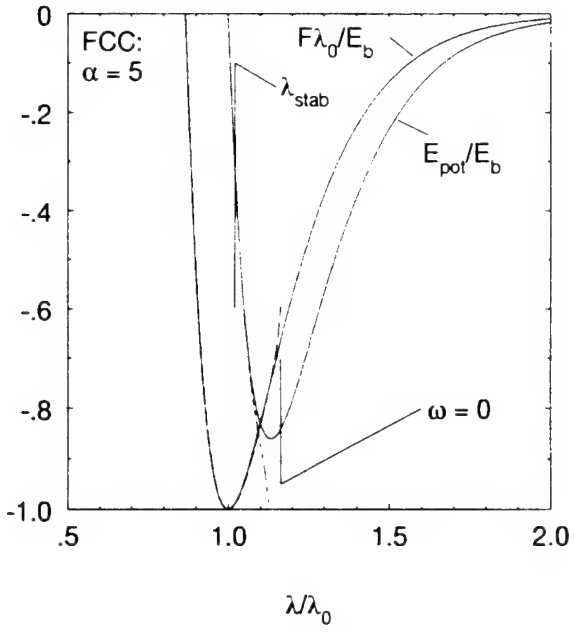

(c)

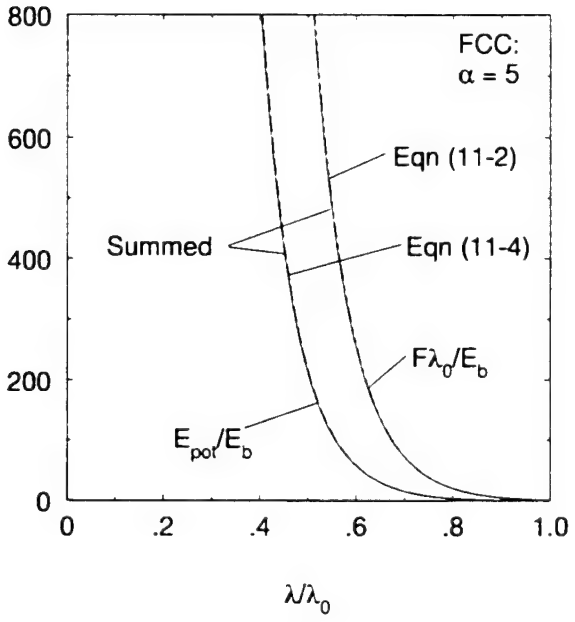

(d)

Figure 10. A comparison of the lattice's energy potential and force (solid lines) to the analytical, frequency-based result (dashed lines): (a) FCC, $\alpha = 2$ (expansion); (b) FCC, $\alpha = 2$ (compression); (c) FCC, $\alpha = 5$ (expansion); (d) FCC, $\alpha = 5$ (compression). Shown on (a) and (c) are lattice spacings corresponding to λ_{stab} and $\omega = 0$.

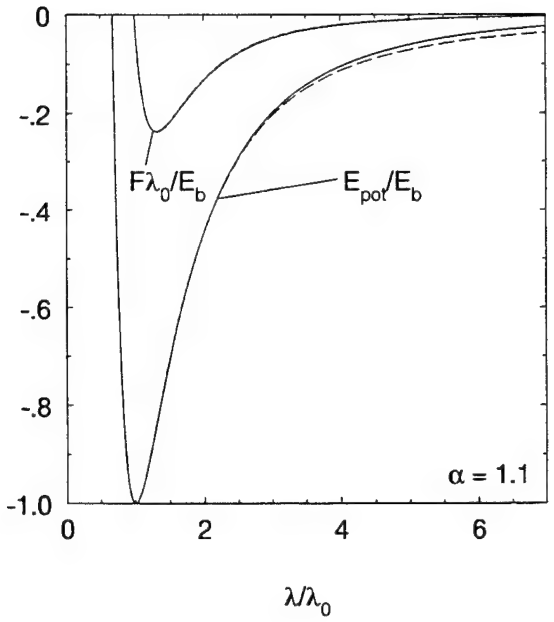

Figure 11. A comparison of the summed energy and lattice force (solid lines) to the analytical forms of eqns (11–3) and (11–4) (dashed lines), for the FCC case of very low $\alpha = 1.1$.

eqn (11–2), and not as an end unto itself]. To determine κ, we may add the individual calculations of β and ξ, eqns (9–2) and (10–2), which has the effect of defining κ to match the curvature of F at the reference state. When κ is computed in this manner, it may be explicitly defined as

$$\kappa = [\Gamma_{vol0} + 1 - 3/2 \cdot \Gamma_0 (d\psi/dV)_0]/\Gamma_0 \quad . \tag{11–5}$$

Computed values for κ (and for comparison, K) are given in Table 5, for a variety of lattice conditions. Note that, were κ to take on the value of K, eqn (11–1) would be recovered from (11–4). Similarly, as $\omega \rightarrow 0$, E_c does not, in general, approach E_b, but rather $E_b (K/\kappa)^2$. Since Table 5 shows the values for K and κ converging at low α, however, we might conclude that, in the low-anharmonicity limit, the analytical form should match the summed potential all the way to $E_c = E_b$, which corresponds to $\lambda \rightarrow \infty$. We, in fact, noted this apparent trend in Figure 11.

One last point to note is that eqn (11–3) actually provides an even better fit to the triple-summed lattice-force equations than does eqn (9–1), from which it derives. Presumably, the

Table 5. Values for Parameters[a] K and κ

α	K (κ)		
	SC[b]	BCC	FCC
1.1	1.23 (1.26)	1.26 (1.27)	1.26 (1.28)
1.5	1.22 (1.30)	1.30 (1.34)	1.31 (1.35)
2	1.19 (1.36)	1.29 (1.42)	1.31 (1.43)
2.5	1.16 (1.42)	1.27 (1.48)	1.29 (1.49)
3	1.13 (1.46)	1.25 (1.53)	1.27 (1.53)
4	1.09 (1.54)	1.20 (1.59)	1.22 (1.59)
5	1.05 (1.59)	1.18 (1.63)	1.18 (1.63)

[a] Computed from principal stiffnesses only.

[b] For simple cubic lattice, computed from longitudinal stiffness only, as SC lattice not stable in shear, along the principal lattice directions.

approximations in the functional behavior of ψ, used to derive eqn (11–3), compensated somewhat for the deviation noted in eqn (9–1) at the higher interaction decay-rates.

Since the current modeling has $\Gamma = \Gamma(V)$, which results from the fact that the vibrational stiffness was not modeled to be temperature dependent, the current results may be cast in the Grüneisen equation-of-state form:

$$p\psi - E = p_c\psi - E_c \quad . \tag{11–6}$$

Substituting eqns (11–3) and (11–4) into eqn (11–6) gives the following equation of state:

$$p\psi - E = B_0 V_0/(\Gamma_0 \kappa)^2 \{[(\omega/\omega_0)^\kappa - 1] + \kappa(\kappa - 1)(\omega/\omega_0)^\kappa \ln(\omega/\omega_0)\} \quad . \tag{11–7}$$

12. Comparison to Data

As the first step in testing the merits of eqn (11–7), we will choose to compute various thermodynamic curves from eqn (11–7) [or eqn (11–3) from which it derives] and compare these results to experimental data. Since these equations are not a function of λ or V, we must, somehow, relate them back to lattice spacing in order to actually accomplish the comparison. The simplest approach would be to assume the validity of eqn (10–3), which amounts to assuming a functional form for Γ. The real behavior of ψ is, no doubt, more complicated than this polynomial form, and one could expect to achieve improved comparisons to data by customizing a fit to ψ for each given case. Nonetheless, rather than adopting a customized ψ function, the assumption of eqn (10–3), along with a fit to the single parameter ξ, should provide immediate feedback on whether the modeling approach is on the right track.

For the case already considered, that of specifying a pairwise potential for a lattice, all of the parameters required to evaluate the merits of eqn (11–7) are available from the triple-summation equations for the lattice energy, force, and stiffnesses. To evaluate eqn (11–7) for an actual crystalline material where the pairwise potential is not known, however, requires the

acquisition of the various model parameters by other means. Required of the model are values for a number of parameters at the equilibrium state. Many of them, such as B_0 and V_0, are handbook values [furthermore, only their product, defining the bulk sound speed via $C_0 = (B_0 V_0)^{1/2}$, appears in the model]. Others, such as Γ_0, are widely reported in the literature as well, though these reported values may vary somewhat from source to source. For the volumetric anharmonicity, Γ_{vol0}, we use the approximate rule of thumb (reported here in section 8) that $\Gamma_{vol0} = \eta/2.6$, since values for η are provided for many materials by Rose *et al.* [11]. In the future, more precise methods may be employed to directly measure the curvature of the equilibrium lattice force. Finally, in order to obtain κ by way of eqn (11–5), a value of $(d\psi/dV)_0$ is required. Though such a value is obtainable from material conditions at the equilibrium state, there has been little or no occasion to report such data in the literature. Therefore, we choose to estimate this parameter by selecting a value of ξ (hopefully) in the vicinity of 0.5, and employing eqn (10–2) to evaluate $(d\psi/dV)_0$ as

$$(d\psi/dV)_0 = 4/(3\,\Gamma_0) - \xi \quad . \tag{12–1}$$

With all the parameters required of the model now obtainable, we may proceed with a few representative comparisons. We will accomplish the comparisons by calculating both the cold-compression curve and shock Hugoniot for several materials. The cold-compression curve is a direct test of eqn (11–3) in the absence of thermal effects. The shock Hugoniot, by contrast, is a function of both the mechanical and the thermal properties of the lattice. It may be obtained by eliminating E from eqn (11–7) by way of the Rankine-Hugoniot shock-energy relation

$$E - E_0 = (p_0 + p)(V_0 - V)/2 \quad , \tag{12–2}$$

which governs internal energy across a shock wave. For the reference Hugoniot originating from the equilibrium lattice condition, both E_0 and p_0 are zero.

The quality of this match will test not only eqn (9–1) but also the observed correlation of eqn (10–1), both of which have fed into the formulation of eqns (11–3), (11–4), and,

ultimately, (11–7). Comparisons to silver, aluminum, copper, and stainless steel are shown in Figures 12–15, with the corresponding parameters given in Table 6. The comparisons to both the cold-compression and shock-Hugoniot data for these representative materials are very good to a number of megabars of compression before, in some cases, diverging. And as said previously, the application of a more general form on ψ, in preference to the assumed form of eqn (10–3), can further improve the correlation to data. The purpose, however, in retaining the simplified assumption of eqn (10–3) is merely to demonstrate the general validity of the method and approach, as laid out in this paper. Further refinements to the model, with the intent to improve correlations to data, would, at this time, serve only to obfuscate the simplicity of this introductory report, which lays out a static-atomic paradigm for lattice vibration. Perhaps of more importance, however, is the fact that above several (1 to 2) megabars of pressure, Mitchell *et al.* [26] note that shocked metals are prone to melting. We might therefore expect that a model, such as the present one, which presumes the material to remain in the solid state, might no longer calibrate to the very high shock pressure data.

Table 6. Parameters for Experimental Comparison

	$C_0 = (B_0 V_0)^{1/2}$ (m/s)	$1/V_0$ (kg/m^3)	Γ_0	Γ_{vol0} [a]	ξ	κ [b]	$(d\psi/dV)_0$ [c]
Ag	3221	10490	2.22	2.29	0.500	1.33	0.10
Al	5189	2700	2.03	1.84	0.716	1.49	–0.06
Cu	3995	8930	2.02	2.10	0.520	1.32	0.14
St. Steel	4571	7896	1.81	2.00	0.550	1.38	0.19

[a] Selected in vicinity of $\Gamma_{vol0} = \eta/2.6$. Values for η obtained from Rose *et al.* [11].
[b] Computed by way of eqn (11–5).
[c] Computed by way of eqn (12–1).

We take brief pause, however, to consider one difference noted between the analysis and the experimental data—and that is the generally low values of Γ_0 computed in Table 3. An examination of the modes constituting ψ, as shown in Figure 5, can shed some light on this subject. From this figure, we note that the transverse mode is more stable than the longitudinal

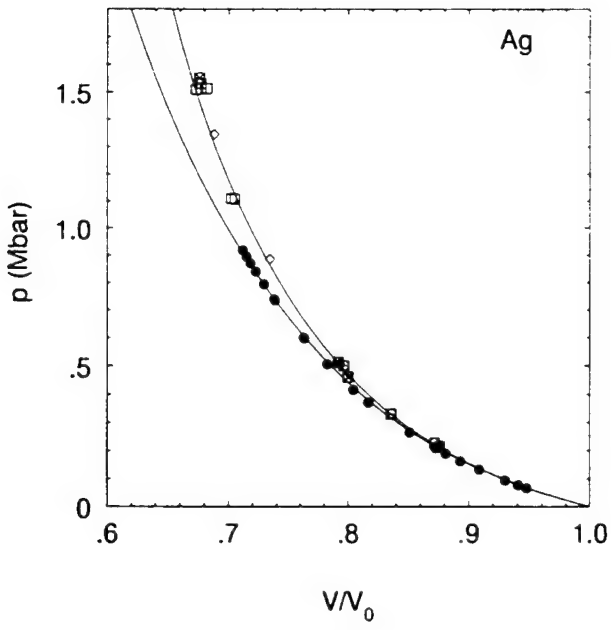

(a)

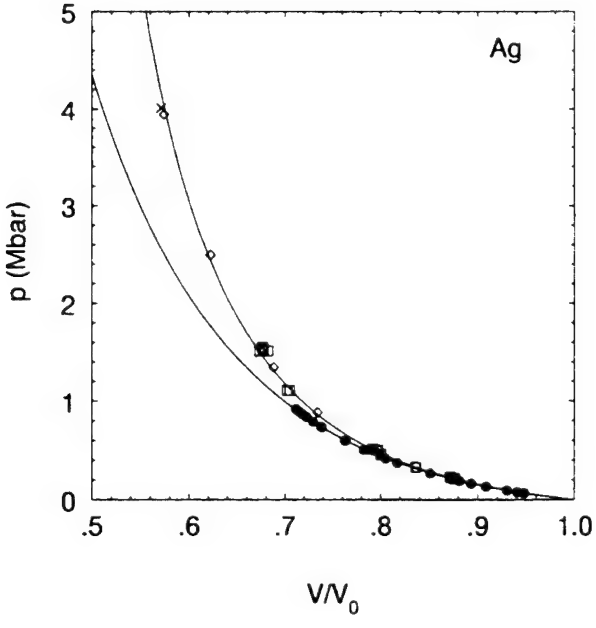

(b)

Figure 12. The cold-compression and shock-Hugoniot curves for silver: (a) to 1.8 megabars; (b) to 5 megabars. Note that cold-compression data [21] are filled symbols and Hugoniot data [22, 23] are open symbols.

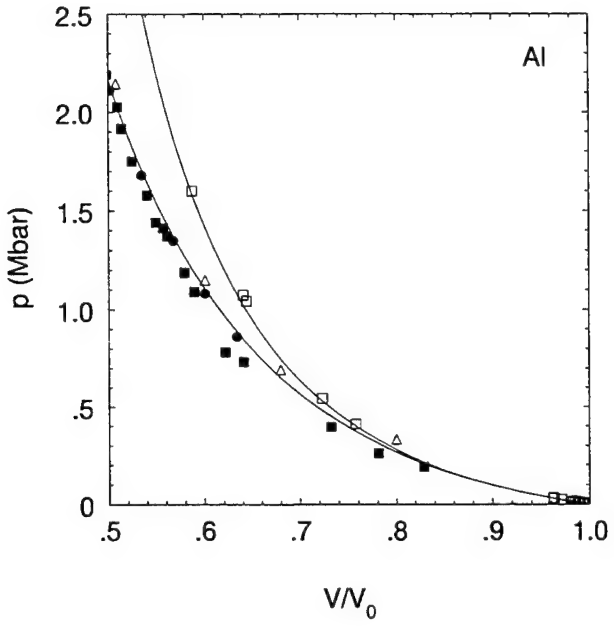

(a)

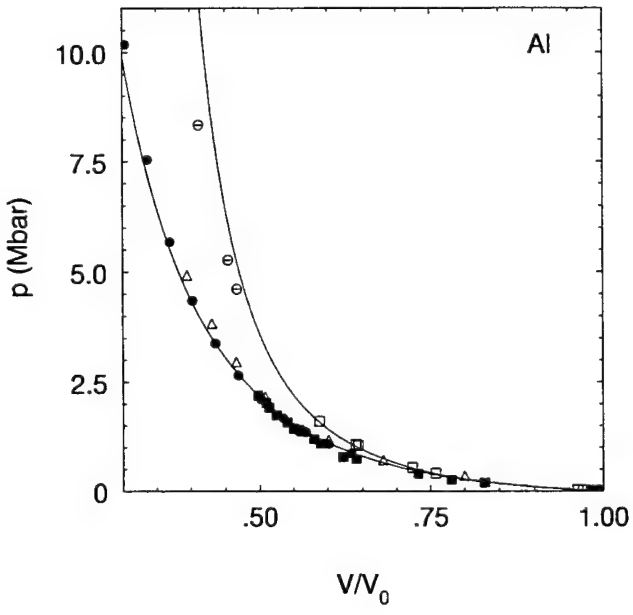

(b)

Figure 13. The cold-compression and shock-Hugoniot curves for aluminum: (a) to 2.5 megabars; (b) to 11 megabars. Note that cold-compression data [16, 24, 25] are filled symbols and Hugoniot data [23, 26] are open symbols.

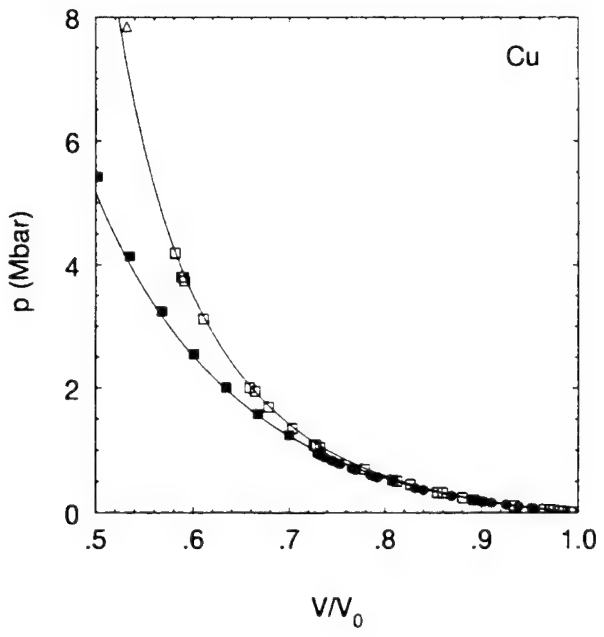

(a)

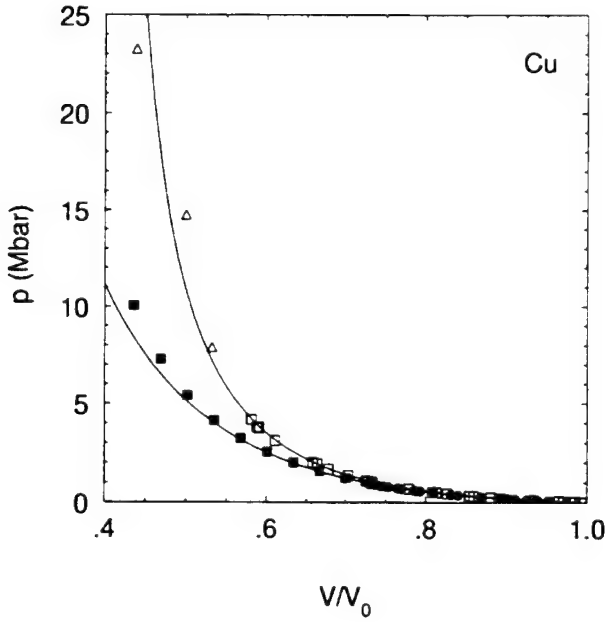

(b)

Figure 14. The cold-compression and shock-Hugoniot curves for copper: (a) to 8 megabars; (b) to 25 megabars. Note that cold-compression data [21, 24] are filled symbols and Hugoniot data [23, 26] are open symbols.

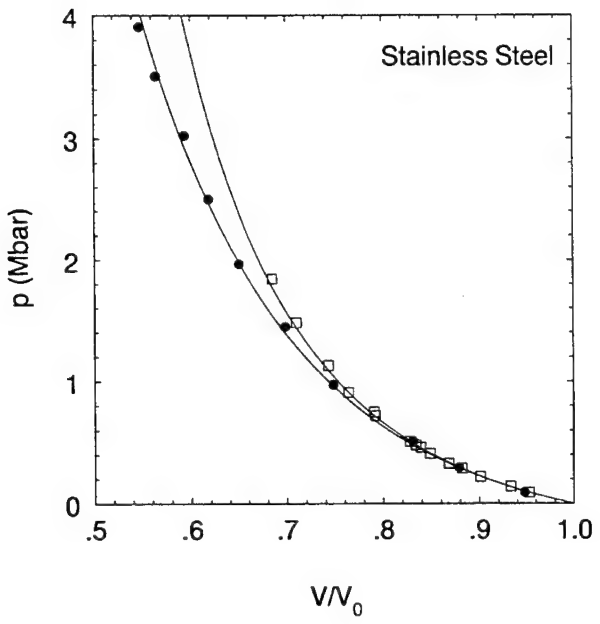

Figure 15. The cold-compression- and shock-Hugoniot curves for stainless steel to 4 megabars. Note that cold-compression data [11] are filled symbols and Hugoniot data [23] are open symbols.

one, in that ψ_T remains defined to a larger λ than does ψ_L. Let us keep in mind, here, that the L and T modes employed in this analysis represent but three of the many frequency modes of the lattice and that, in reality, the true ψ will be composed of all the frequency modes and not just these three.

The makeup of the aggregation relation, eqn (7–1), is such that as soon as any vibrational mode goes unstable ($\omega_i \rightarrow 0$), the aggregated ω must do so as well. And though the behavior of the aggregated ψ tracks the more stable (larger) ψ_T at larger compressions, we do, in fact, see that ψ tracks the less stable ψ_L at expansions beyond λ_{stab}, the maximum in the ψ curve. If there exists in the lattice a mode less stable than the principal L mode considered in this report, then the aggregated ψ should instead track that least-stable mode as the lattice expansion approaches the stability limit of $\omega \rightarrow 0$. The net effect of the modal coupling of eqn (7–1) is that, when moving from a compressed lattice state to one of expansion, ψ begins to deviate from the component ψ associated with the most-stable mode of the lattice, and asymptotes to the behavior of the least-stable lattice mode.

The lowering of ψ with increased λ, arising from the influence of the least stable lattice mode, amounts to a net increase in Γ over what the stable mode would have established (since $\Gamma = V/\psi$). The fact that values for Γ_0, as calculated in Table 3, are lower than comparable experimental values allows us to conclude that the principal L vibrational mode considered in this study was not the least-stable mode of the lattice. Whereas we see little deviation between ψ and ψ_T, in Figure 5, at the λ_0 reference condition (ψ_L only exerts profound influence at larger expansions), the higher values of Γ provided by experimental data suggest that the least-stable mode, in reality, is already influencing ψ at the reference state, λ_0. This brief analysis suggests that future efforts along this line of attack might provide improved results by examining the least and most stable lattice modes, as opposed to the modes associated with the principal directions of the lattice structure.

13. Conclusions

This report details a simple, static-atomic approach for computing the characteristic vibrational behavior of an atomic lattice, when the properties of the pairwise interaction are given. At the core of the method is the understanding that, when atomic interactions are accounted for beyond the extent of nearest neighbors, the vibrational and volumetric stiffnesses are, by necessity, functionally distinct. Such a distinction is at odds with virtually all prior analytical treatments of the subject [2, 5, 6–9], perhaps because accounting for the interactions of nonnearest neighbors in three dimensions has, before now, never been achievable in a straighforward, simple manner. Admittedly, the stiffness is computed along only the principal axes of the lattice and so anisotropy in the stiffness is not accounted for. Nonetheless, these limitations are the same employed in a number of earlier analyses on the subject [2, 5]—analyses that have proved valuable.

The results of employing the method are equations involving triple summations, which are able to provide the lattice potential, interatomic force, volumetric- and characteristic-vibrational stiffnesses, as well as the Grüneisen function for the lattice—in essence, the complete equation of state for the material. An analysis was performed to show how the mechanical behavior of the lattice compares to the behavior of the constituent pairwise interaction. Results also confirmed the distinct functional nature of the volumetric and vibrational stiffnesses of the lattice.

By examining the current results in light of a recently published semi-empirical model, the triple-summation equation for lattice force could be cast in a closed-form analytical equation, in terms of the characteristic vibrational behavior of the lattice, and without the use of fitting parameters. The thermal properties of the computed lattice were shown, and an empirical correlation was observed between the characteristic vibrational frequency of the lattice and its derivative. This correlation seemed valid, over a wide range of stiffnesses, for all but the largest expansions and vanishingly small compressions. The correlation, when adopted, translates into analytically specifiable functional forms for Γ, ψ, and ω.

When the analytical functional form put forth for the mechanical force in the lattice is combined with the correlation found to govern the thermal properties of the lattice, a comprehensive, thermal equation of state is established. This equation, it turns out, is identical in form to the recently proposed semi-empirical form [10], but for the value of a single exponent. Because the form of the equation of state is in terms of the characteristic vibrational frequency of the lattice, this analytical equation of state is only valid at states where the characteristic frequency is defined. The current analysis has determined that, at some level of expansion beyond the inflection point of the lattice potential, the vibrational stiffness changes sign and, thus, the characteristic vibrational frequency becomes undefined. Therefore, the analytical equation of state proposed will be unable to make thermodynamic predictions for lattice separations beyond this critical value of lattice spacing.

A comparison of the analytical equation of state was performed against cold-compression and shock-Hugoniot data for several materials. Without a given pairwise interaction known to govern the behavior of the lattice, and because the model is a function only of the lattice's vibrational frequency and its derivatives, an assumption had to be made about the the manner in which the vibrational frequency varies with lattice spacing. The assumption adopted was the simplest possible—namely, that the vibrational behavior of the actual lattice was identical in form to that noted (in the pairwise-interaction study) by the correlation of eqn (10–1). That assumption requires the specification of a single scalar parameter, which is known to lie in the vicinity of 1/2 (the low-anharmonicity limit for the parameter). Though better correlations with data are obtainable by deviating from this assumption, the assumption was nonetheless retained, to highlight both the simplicity of the model and its ability to predict the compressive and thermal behavior of an actual lattice over a wide change in volume, corresponding to several megabars of pressure.

14. References

1. Born, M., and T. von Karman. "Über Schwingungen in Raumgittern." *Physikalische Zeitschrift*, **13** (8), pp. 297–309, 1912.

2. Slater, J.C. *Introduction to Chemical Physics*. McGraw Hill: New York, 1939.

3. Plendl, J.N. "Some New Interrelations in the Properties of Solids Based on Anharmonic Cohesive Forces." *Physical Review*, **123** (4), pp. 1172–1180, 1961.

4. Plendl, J.N. "New Concepts in the Physics of Solids: A Monograph." AFCRL-66-541, Air Force Cambridge Research Laboratories, Bedford, Massachusetts, August 1966.

5. Dugdale, J.S., and D.K.C. McDonald. "The Thermal Expansion of Solids." *Physical Review*, **89** (4), pp. 832–834, 1953.

6. Pastine, D.J. "Formulation of the Grüneisen Parameter for Monatomic Cubic Crystals." *Physical Review*, **138** (3A), pp. A767–A770, 1965.

7. Vashchenko, V.Y., and V.N. Zubarev. "Concerning the Grüneisen Constant." *Soviet Physics—Solid State*, **5** (3), pp. 653–655, 1963.

8. Brillouin, L. *Wave Propagation in Periodic Structures*. New York: Dover, 1953. Originally published by New York: McGraw Hill, 1946.

9. Guinea, F., J.H. Rose, J.R. Smith, and J. Ferrante. "Scaling Relations in the Equation of State, Thermal Expansion, and Melting of Metals." *Applied Physics Letters*, **44** (1), pp. 53–55, 1984.

10. Segletes, S.B. "A Frequency-Based Equation of State for Metals." *International Journal of Impact Engineering*, accepted for publication, 1998.

11. Rose, J.H., J.R. Smith, F. Guinea, and J. Ferrante. "Universal Features of the Equation of State of Metals." *Physical Review B*, **29** (6), pp. 2963–2969, 1984.

12. Segletes, S.B., and W.P. Walters. "On Theories of the Grüneisen Parameter." *Journal of Physics and Chemistry of Solids*, **59** (3), pp. 425–433, 1998.

13. Segletes, S.B. "Elastic Behavior of an Atomic Lattice Under Large Volumetric Strains: The Quasi-Harmonic Idealization." ARL-TR-1357, U.S. Army Research Laboratory, Aberdeen Proving Ground, Maryland, May 1997.

14. Segletes, S.B. "Regarding the Frequency-Based Equation of State of Segletes." ARL-TR-1403, U.S. Army Research Laboratory, Aberdeen Proving Ground, Maryland, June 1997.

15. Schulte, O., and W.B. Holzapfel. "Effect of Pressure on Atomic Volume and Crystal Structure of Indium to 67 GPa." *Physical Review B*, **48** (2), pp. 767–773, 1993.

16. Greene, R.G., H. Luo, and A.L. Ruoff. "Al as a Simple Solid: High Pressure Study to 220 GPa (2.2 Mbar)." *Physical Review Letters*, **73** (15), pp. 2075–2078, 1994.

17. Vinet, P., J.R. Smith, J. Ferrante, and J.H. Rose. "Temperature Effects on the Universal Equation of State of Solids." *Physical Review B*, **35** (4), pp. 1945–1953, 1987.

18. Syassen, K., and W.B. Holzapfel. "Isothermal Compression of Al and Ag to 120 kbar." *Journal of Applied Physics*, **49** (8), pp. 4427–4430, 1978.

19. Baonza, V.G., M. Cáceres, and J. Núnez. "Universal Compressibility Behavior of Dense Phases." *Physical Review B*, **51** (1), pp. 28–37.

20. Segletes, S.B. "The Effect of Thermodynamic Constraints upon the Mie-Grüneisen Equation of State" in *Constitutive Laws*. A.M. Rajendran, R.C. Batra (eds.), CIMNE: Barcelona, pp. 46–51, 1995.

21. Mao, H.K., P.M. Bell, J.W. Shaner, and D.J. Steinberg. "Specific Volume Measurements of Cu, Mo, Pd, and Ag and Calibration of the Ruby R_1 Fluoresence Pressure Gauge From 0.06 to 1 Mbar." *Journal of Applied Physics*, **49** (6), pp. 3276–3283, 1978.

22. van Thiel, M., A.S. Kusibov, and A.C. Mitchell (eds.). "Lawrence Radiation Laboratory Compendium of Shock Wave Data." UCRL-50108, University of California, Livermore, California, 1967.

23. Kohn, B.J. "Compilation of Hugoniot Equations of State." AFWL-TR-69-38, U.S. Air Force Weapons Laboratory, Kirtland AFB, New Mexico, April, 1969.

24. Nellis, W.J., J.A. Moriarty, A.C. Mitchell, M. Ross, R.G. Dandrea, N.W. Ashcroft, N.C. Holmes, and G.R. Gathers. "Metals Physics at Ultrahigh Pressure: Aluminum, Copper, and Lead as Prototypes." *Physical Review Letters*, **60** (14), pp. 1414–1417, 1988.

25. Molodets, A.M. "Grüneisen Function and the Zero-Temperature Isotherm of Three Metals up to Pressures of 10 TPa." *JETP*, **80** (3), pp. 467–471, 1995.

26. Mitchell, A.C., W.J. Nellis, J.A. Moriarty, R.A. Heinle, N.C. Holmes, R.E. Tipton, and G.W. Repp. "Equation of State of Al, Cu, Mo, and Pb at Shock Pressures up to 2.4 TPa (24 Mbar)." *Journal of Applied Physics*, **69** (5), pp. 2981–2986, 1991.

27. Segletes, S.B. "A Compact Analytical Fit to the Exponential Integral $E_1(x)$." ARL-TR-1758, U.S. Army Research Laboratory, Aberdeen Proving Ground, Maryland, September 1998.

NO. OF COPIES ORGANIZATION

2 DEFENSE TECHNICAL INFORMATION CENTER
DTIC DDA
8725 JOHN J KINGMAN RD
STE 0944
FT BELVOIR VA 22060-6218

1 HQDA
DAMO FDQ
DENNIS SCHMIDT
400 ARMY PENTAGON
WASHINGTON DC 20310-0460

1 OSD
OUSD(A&T)/ODDDR&E(R)
R J TREW
THE PENTAGON
WASHINGTON DC 20301-7100

1 CECOM
SP & TRRSTRL COMMCTN DIV
AMSEL RD ST MC M
H SOICHER
FT MONMOUTH NJ 07703-5203

1 PRIN DPTY FOR TCHNLGY HQ
US ARMY MATCOM
AMCDCG T
M FISETTE
5001 EISENHOWER AVE
ALEXANDRIA VA 22333-0001

1 DPTY CG FOR RDE HQ
US ARMY MATCOM
AMCRD
BG BEAUCHAMP
5001 EISENHOWER AVE
ALEXANDRIA VA 22333-0001

1 INST FOR ADVNCD TCHNLGY
THE UNIV OF TEXAS AT AUSTIN
PO BOX 202797
AUSTIN TX 78720-2797

1 GPS JOINT PROG OFC DIR
COL J CLAY
2435 VELA WAY STE 1613
LOS ANGELES AFB CA 90245-5500

NO. OF COPIES ORGANIZATION

1 DARPA
B KASPAR
3701 N FAIRFAX DR
ARLINGTON VA 22203-1714

1 NAVAL SURFACE WARFARE CTR
CODE B07 J PENNELLA
17320 DAHLGREN RD
BLDG 1470 RM 1101
DAHLGREN VA 22448-5100

1 US MILITARY ACADEMY
MATH SCI CTR OF EXCELLENCE
DEPT OF MATHEMATICAL SCI
MDN A MAJ DON ENGEN
THAYER HALL
WEST POINT NY 10996-1786

1 DIRECTOR
US ARMY RESEARCH LAB
AMSRL CS AL TA
2800 POWDER MILL RD
ADELPHI MD 20783-1145

3 DIRECTOR
US ARMY RESEARCH LAB
AMSRL CI LL
2800 POWDER MILL RD
ADELPHI MD 20783-1145

ABERDEEN PROVING GROUND

4 DIR USARL
AMSRL CI LP (305)

NO. OF COPIES	ORGANIZATION
1	US ARMY DUSA OPS RSCH ATTN DANIEL WILLARD 102 ARMY PENTAGON WASHINGTON DC 20310-0102
5	DEFENSE NUCLEAR AGENCY ATTN MAJ JAMES LYON CDR KENNETH W HUNTER TONY FREDERICKSON R JEFFREY LAWRENCE SPSP KIM KIBONG 6801 TELEGRAPH RD ALEXANDRIA VA 22310-3398
3	COMMANDER US ARMY ARDEC ATTN AMSTA AR FSA E W P DUNN J PEARSON E BAKER PICATINNY ARSENAL NJ 07806-5000
1	COMMANDER US ARMY ARDEC ATTN AMSTA AR CCH V M D NICOLICH PICATINNY ARSENAL NJ 07806-5000
1	COMMANDER US ARMY ARDEC ATTN E ANDRICOPOULOS PICATINNY ARSENAL NJ 07806-5000
1	COMMANDER USA STRATEGIC DEFNS CMD ATTN CSSD H LL T CROWLES HUNTSVILLE AL 35807-3801
2	COMMANDER US ARMY MICOM ATTN AMSMI RD ST WF D LOVELACE M SCHEXNAYDER REDSTONE ARSENAL AL 35898-5250
1	MIS DEFNS & SPACE TECHNOLOGY ATTN CSSD SD T KENNETH H JORDAN PO BOX 1500 HUNTSVILLE AL 34807-3801

NO. OF COPIES	ORGANIZATION
4	COMMANDER US ARMY BELVOIR RD&E CTR ATTN STRBE NAE B WESTLICH STRBE JMC T HANSHAW STRBE NAN S G BISHOP J WILLIAMS FORT BELVOIR VA 22060-5166
3	COMMANDER US ARMY RESEARCH OFFICE ATTN J CHANDRA K IYER J BAILEY PO BOX 12211 RESEARCH TRIANGLE PARK NC 27709-2211
1	DIRECTOR NAVAL CIVIL ENGRNG LAB ATTN J YOUNG CODE L56 PORT HUENEME CA 93043
1	NAVAL POSTGRADUATE SCHOOL PHYSICS DEPARTMENT ATTN JOSEPH STERNBERG MONTEREY CA 93943
1	NAVAL AIR WARFARE CTR ATTN STEPHEN A FINNEGAN BOX 1018 RIDGECREST CA 93556
3	COMMANDER NAVAL WEAPONS CENTER ATTN T T YEE CODE 3263 D THOMPSON CODE 3268 W J MCCARTER CODE 6214 CHINA LAKE CA 93555

NO. OF COPIES	ORGANIZATION
12	COMMANDER NAVAL SURFACE WARFARE CTR DAHLGREN DIVISION ATTN H CHEN D L DICKINSON CODE G24 CHARLES R ELLINGTON C R GARRETT CODE G22 W HOLT CODE G22 R MCKEOWN W WALLACE MORTON JR JOHN M NELSON M J SILL CODE H11 WILLIAM J STROTHER A B WARDLAW, JR. L F WILLIAMS CODE G33 17320 DAHLGREN RD DAHLGREN VA 22448
5	AIR FORCE ARMAMENT LAB ATTN AFATL DLJW W COOK M NIXON AFATL DLJR J FOSTER AFATL MNW LT D LOREY R D GUBA EGLIN AFB FL 32542
1	USAF PHILLIPS LABORATORY VTSI ATTN ROBERT ROYBAL KIRTLAND AFB NM 87117-7345
2	USAF PHILLIPS LABORATORY ATTN PL WSCD FIROOZ ALLAHDADI PV VTA DAVID SPENCER 3550 ABERDEEN AVE SE KIRTLAND AFB NM 87117-5776
5	WRIGHT LABS ATTN MNMW JOEL W HOUSE ARMAMENT DIRECTORATE STE 326 B1 RONALD D HUNT BRYAN MILLIGAN BRUCE C PATTERSON WADE H VAUGHT 101 W EGLIN BLVD EGLIN AFB FL 32542-6810

NO. OF COPIES	ORGANIZATION
1	AFIT ENC ATTN DAVID A FULK WRIGHT PATTERSON AFB OH 45433
42	DIRECTOR LANL ATTN M LUCERO MS A105 J V REPA MS A133 J P RITCHIE MS B214 T14 R DINGUS MS B218 N KRIKORIAN MS B228 R KIRKPATRICK MS B229 R THURSTON MS B229 C T KLINGNER MS B294 R MILLER MS B294 B SHAFER MS C931 G GISLER MS D436 C RAGAN MS D449 B LAUBSCHER MS D460 M O SCHNICK MS F607 R WELLS MS F607 R KOPP MS F645 R STELLINGWERFMS F645 C WINGATE MS F645 T ADAMS MS F663 R GODWIN MS F663 K JACOBY MS F663 W SPARKS MS F663 E J CHAPYAK MS F664 J SHANER MS F670 G CANAVAN MS F675 R GREINER MS G740 J HILLS MS G770 B HOGAN MS G770 J BOLSTAD MS G787 J WALSH MS G787 R DAVIDSON MS K557 R HENNINGER MS K557 N6 T ROLLET MS K574 P HOWE MS P915 W DEAL MS P915 J KENNEDY MS P915 A ROACH MS P915 W HEMSING MS P940 E POGUE MS P940 J MCAFEE MS P950 D PAISLEY MS P950 L PICKLESIMER MS P950 PO BOX 1663 LOS ALAMOS NM 87545

NO. OF COPIES	ORGANIZATION
6	DIRECTOR LANL ATTN R WARNES MS P950 S SHEFFIELD MS P952 D MANDELL K MARK S J MOSSO L SCHWALBE PO BOX 1663 LOS ALAMOS NM 87545
35	DIRECTOR SANDIA NATL LABS ATTN E H BARSISMS-031 ERIC W REECE MS-0307 DANIEL P KELLYMS-0307 L WEIRICK MS-0327 R TACHAU MS-0425 D LONGCOPE MS-0439 D HAYES MS-0457 J ASAY MS-0458 W TEDESCHI MS-0482 J SCHULZE MS-0483 P A LONGMIREMS-0560 J COREY MS-0576 E S HERTEL JRMS-0819 A ROBINSON MS-0819 T TRUCANO MS-0819 J M MCGLAUN MS-0819 R BRANNON MS-0820 L CHHABILDASMS-0821 J ANG MS-0821 M BOSLOUGH MS-0821 L CHHABILDAS MS-0821 D CRAWFORD MS-0821 M FURNISH MS-0821 C HALL MS-0821 W REINHART MS-0821 P STANTON MS-0821 M KIPP DIV 1533 P YARRINGTON DIV 1533 J MCGLAWA DIV 1541 M FORRESTAL DIV 1551 R LAFARGE DIV 1551 C HILLS DIV 1822 R O NELLUMS DIV 9122 P TAYLOR ORG 1432 D KERNAN ORG 1433 PO BOX 5800 ALBUQUERQUE NM 87185

NO. OF COPIES	ORGANIZATION
6	DIRECTOR SANDIA NATL LABS ATTN B LEVIN ORG 7816 L N KMETYK R REEDER J SOUTHWARD C KONRAD K LANG PO BOX 5800 ALBUQUERQUE NM 87185
3	DIRECTOR LLNL MS L35 ATTN R E TIPTON D BAUM T MCABEE PO BOX 808 LIVERMORE CA 94550
7	DIRECTOR LLNL MS L122 ATTN R PIERCE R ROSINKY O J ALFORD D STEWART T VIDLAK B R BOWMAN W DIXON PO BOX 808 LIVERMORE CA 94550
2	DIRECTOR LLNL MS L125 ATTN DOUGLAS R FAUX NORMAN W KLINO PO BOX 808 LIVERMORE CA 94550
1	DIRECTOR LLNL ATTN ROBERT BARKER L159 PO BOX 808 LIVERMORE CA 94550

NO. OF COPIES	ORGANIZATION
3	DIRECTOR LLNL MS L163 ATTN MILTON FINGER R PERRET W SHOTTS PO BOX 808 LIVERMORE CA 94550
3	DIRECTOR LLNL MS L178 ATTN H KRUGER G POMYKAL MICHAEL GERASSIMENKO PO BOX 808 LIVERMORE CA 94550
2	DIRECTOR LLNL MS L180 ATTN G SIMONSON A SPERO PO BOX 808 LIVERMORE CA 94550
1	DIRECTOR LLNL ATTN FRANK A HANDLER L182 PO BOX 808 LIVERMORE CA 94550
2	DIRECTOR LLNL MS L282 ATTN W TAO P URTIEW PO BOX 808 LIVERMORE CA 94550
2	DIRECTOR LLNL MS L290 ATTN A HOLT J E REAUGH PO BOX 808 LIVERMORE CA 94550

NO. OF COPIES	ORGANIZATION
1	DIRECTOR LLNL ATTN W J NELLIS L299 PO BOX 808 LIVERMORE CA 94550
1	DIRECTOR LLNL ATTN D WOOD L352 PO BOX 808 LIVERMORE CA 94550
1	DIRECTOR LLNL ATTN STEPHEN G COCHRAN L389 PO BOX 808 LIVERMORE CA 94550
3	DIRECTOR LLNL MS L495 ATTN D GAVEL J HUNTER E JOHANSSON PO BOX 808 LIVERMORE CA 94550
1	DIRECTOR LLNL ATTN R M KUKLO L874 PO BOX 808 LIVERMORE CA 94550
8	DIRECTOR LLNL ATTN G W REPP M J MURPHY A C MITCHELL J A MORIARTY R A HEINLE N C HOLMES M SHANNON BMDO ROBERT M HALL PO BOX 808 LIVERMORE CA 94550

NO. OF COPIES	ORGANIZATION
3	ENERGETIC MATERIALS RSCH CTR/DOE NEW MEXICO INST OF MINING & TECH ATTN DAVID J CHAVEZ LARRY LIBERSKY FRED SANDSTROM CAMPUS STATION SOCORRO NM 87801
1	NASA LEWIS RESEARCH CENTER ATTN J FERRANTE CLEVELAND OH 44135
3	NASA JOHNSON SPACE CENTER ATTN ERIC CHRISTIANSEN JEANNE LEE CREWS FREDRICH HORZ MAIL CODE SN3 2101 NASA RD 1 HOUSTON TX 77058
1	APPLIED RESEARCH LAB ATTN JEFFREY A COOK 10000 BURNETT ROAD AUSTIN TX 78758
1	GM RESEARCH LABS ATTN J R SMITH WARREN MI 48090
5	JET PROPULSION LABORATORY IMPACT PHYSICS GROUP ATTN ZDENEK SEKANINA PAUL WEISSMAN BOB WEST JAMES ZWISSLER MARC ADAMS 4800 OAK GROVE DR PASADENA CA 91109
1	MIT LINCOLN LAB ARMY SCIENCE BOARD ATTN WADE M KORNEGAY 244 WOOD ST RM S2 139 LEXINGTON MA 02173

NO. OF COPIES	ORGANIZATION
1	BOSTON UNIVERSITY DEPT OF PHYSICS ATTN ZEEV JAEGER 590 COMMONWEALTH AVE BOSTON, MA 02215
2	BROWN UNIVERSITY ATTN R CLIFTON (ENGNG) P SCHULTZ (GEO SCI) PROVIDENCE RI 02912
3	CALTECH ATTN J SHEPHERD MS 105-50 ANDREW P INGERSOLL MS 170-25 THOMAS J AHRENS MS 252-21 1201 E CALIFORNIA BLVD PASADENA CA 91125
1	CALTECH ATTN GLENN ORTON MS 169 237 4800 OAK GROVE DR PASADENA CA 91007
3	CORNELL UNIVERSITY DEPT. MATERIALS SCIENCE & ENGNG ATTN R G GREENE H LUO A L RUOFF ITHACA NY 14853
3	DREXEL UNIVERSITY ATTN MEM DEPT PHYSICS DEPT A ZAVALIANGOS (DEPT MAT ENGNG) 32ND & CHESTNUT ST PHILADELPHIA PA 19104
1	GEORGIA INSTITUTE OF TECHNOLOGY COMPUTATIONAL MODELING CENTER ATTN S ATLURI ATLANTA GA 30332-0356
1	GEORGIA INSTITUTE OF TECHNOLOGY SCHOOL OF MATL SCIENCE & ENGNG ATTN K LOGAN ATLANTA GA 30332-0245

NO. OF COPIES	ORGANIZATION
1	IOWA STATE UNIVERSITY DEPT PHYSICS AND ASTRONOMY ATTN JIM ROSE 34 PHYSICS AMES IA 50011
1	JOHNS HOPKINS UNIVERSITY MAT SCI & ENGNG DEPT ATTN: MO LI 102 MARYLAND HALL 3400 N CHARLES ST BALTIMORE MD 21218-2689
5	JOHNS HOPKINS UNIVERSITY APPLIED PHYSICS LAB ATTN TERRY R BETZER ALVIN R EATON RICHARD H KEITH DALE K PACE ROGER L WEST JOHNS HOPKINS ROAD LAUREL MD 20723
1	LOUISIANA STATE UNIVERSITY ATTN ROBERT W COURTER 948 WYLIE DR BATON ROUGE LA 70808
1	NC STATE UNIVERSITY ATTN YASUYUKI HORIE RALEIGH NC 27695-7908
1	PENNSYLVANIA STATE UNIVERSITY ATTN PHYSICS DEPT UNIVERSITY PARK PA 16802
4	SOUTHWEST RESEARCH INSTITUTE ATTN C ANDERSON S A MULLIN J RIEGEL J WALKER PO DRAWER 28510 SAN ANTONIO TX 78228-0510
1	TEXAS A&M UNIVERSITY PHYSICS DEPARTMENT ATTN DAN BRUTON COLLEGE STATION TX 77843-4242

NO. OF COPIES	ORGANIZATION
1	UC BERKELEY MECHANICAL ENGINEERING DEPT GRADUATE OFFICE ATTN KEZHUN LI BERKELEY CA 94720
1	UC DAVIS INST OF THEORETICAL DYNAMICS ATTN E G PUCKETT DAVIS CA 95616
1	UC LOS ANGELES DEPT OF MAT SCIENCE & ENGNG ATTN J J GILMAN LOS ANGELES CA 90024
2	UC SAN DIEGO DEPT APPL NECH & ENGR SVCS R011 ATTN S NEMAT-NASSER M MEYERS LA JOLLA CA 92093-0411
2	UNIV OF ALA HUNTSVILLE AEROPHYSICS RSCH CTR ATTN GARY HOUGH DAVID J LIQUORNIK PO BOX 999 HUNTSVILLE AL 35899
1	UNIV OF ALA HUNTSVILLE MECH ENGRNG DEPT ATTN W P SCHONBERG HUNTSVILLE AL 35899
1	UNIVERSITY OF CHICAGO DEPT OF THE GEOPHYSICAL SCIENCES ATTN G H MILLER 5734 S ELLIS AVE CHICAGO IL 60637
3	UNIVERSITY OF DAYTON RSCH INST ATTN N BRAR D GROVE A PIEKUTOWSKI 300 COLLEGE PARK DAYTON OH 45469-0182

NO. OF COPIES	ORGANIZATION
4	UNIVERSITY OF DELAWARE DEPT OF MECHANICAL ENGINEERING ATTN PROF J GILLESPIE DEAN R B PIPES PROF J VINSON PROF D WILKINS NEWARK DE 19716
1	UNIVERSITY OF ILLINOIS PHYSICS BUILDING ATTN A V GRANATO URBANA, IL 61801
1	UNIVERSITY OF MARYLAND ATTN PHYSICS DEPT (BLDG 082) COLLEGE PARK MD 20742
1	UNIVERSITY OF PENNSYLVANIA ATTN P A HEINEY DEPT OF PHYSICS & ASTRONOMY 209 SOUTH 33RD ST PHILADELPHIA PA 19104
1	UNIVERSITY OF PUERTO RICO DEPT CHEMICAL ENGINEERING ATTN L A ESTEVEZ MAYAGUEZ PR 00681-5000
1	UNIVERSITY OF TEXAS DEPT OF MECHANICAL ENGINEERING ATTN ERIC P FAHRENTHOLD AUSTIN TX 78712
1	VIRGINIA POLYTECHNIC INSTITUTE COLLEGE OF ENGINEERING ATTN R BATRA BLACKSBURG VA 24061-0219
2	AEROJET ATTN J CARLEONE S KEY PO BOX 13222 SACRAMENTO CA 95813-6000
2	AEROJET ORDNANCE ATTN P WOLF G PADGETT 1100 BULLOCH BLVD SOCORRO NM 87801

NO. OF COPIES	ORGANIZATION
2	ALLIANT TECHSYSTEMS INC ATTN R STRYK G R JOHNSON MN11-1614 600 SECOND ST NE HOPKINS MN 55343
1	MARVIN L ALME 2180 LOMA LINDA DR LOS ALAMOS NM 87544-2769
1	APPLIED RESEARCH ASSOC INC ATTN JEROME D YATTEAU 5941 S MIDDLEFIELD RD SUITE 100 LITTLETON CO 80123
2	APPLIED RESEARCH ASSOC INC ATTN DENNIS GRADY FRANK MAESTAS SUITE A220 4300 SAN MATEO BLVD NE ALBUQUERQUE NM 87110
1	ATA ASSOCIATES ATTN W ISBELL PO BOX 6570 SANTA BARBARA CA 93111
1	BATTELLE ATTN ROBER M DUGAS 7501 S MEMORIAL PKWY SUITE 101 HUNTSVILLE AL 35802-2258
3	BOEING AEROSPACE CO SHOCK PHYSICS & APPLIED MATH ENGINEERING TECHNOLOGY ATTN R HELZER T MURRAY J SHRADER PO BOX 3999 SEATTLE WA 98124
1	BOEING HOUSTON SPACE STN ATTN RUSSELL F GRAVES BOX 58747 HOUSTON TX 77258
1	BRIGS CO ATTN JOSEPH E BACKOFEN 2668 PETERSBOROUGH ST HERNDON VA 20171-2443

NO. OF COPIES	ORGANIZATION
1	CALIFORNIA RSCH & TECHNOLOGY ATTN M MAJERUS PO BOX 2229 PRINCETON NJ 08543
1	CENTURY DYNAMICS INC ATTN N BIRNBAUM 2333 SAN RAMON VALLEY BLVD SAN RAMON CA 94583-1613
1	COMPUTATIONAL MECHANICS CONSULTANTS ATTN J A ZUKAS PO BOX 11314 BALTIMORE MD 21239-0314
1	CYPRESS INTERNATIONAL ATTN A CAPONECCHI 1201 E ABINGDON DR ALEXANDRIA VA 22314
1	DEFENSE TECHNOLOGY INTL. INC ATTN D E AYER THE STARK HOUSE 22 CONCORD ST NASHUA NH 03060
1	DESKIN RESEARCH GROUP INC ATTN EDWARD COLLINS 2270 AGNEW RD SANTA CLARA CA 95054
3	DOW CHEMICAL INC ORDNANCE SYSTEMS ATTN C HANEY A HART B RAFANIELLO 800 BUILDING MIDLAND MI 48667
1	G E DUVALL 5814 NE 82ND COURT VANCOUVER WA 98662-5944
3	DYNA EAST CORP ATTN P C CHOU R CICCARELLI W FLIS 3620 HORIZON DRIVE KING OF PRUSSIA PA 19406
3	DYNASEN ATTN JACQUES CHAREST MICHAEL CHAREST MARTIN LILLY 20 ARNOLD PL GOLETA CA 93117
1	R J EICHELBERGER 409 W CATHERINE ST BEL AIR MD 21014-3613
1	ELORET INSTITUTE ATTN DAVID W BOGDANOFF MS 230 2 NASA AMES RESEARCH CENTER MOFFETT FIELD CA 94035
3	ENIG ASSOCIATES INC ATTN J ENIG D J PASTINE M COWPERTHWAITE SUITE 500 11120 NEW HAMPSHIRE AVE SILVER SPRING MD 20904-2633
1	EXPLOSIVE TECHNOLOGY ATTN M L KNAEBEL PO BOX KK FAIRFIELD CA 94533
1	GB TECH LOCKHEED ATTN JAY LAUGHMAN 2200 SPACE PARK SUITE 400 HOUSTON TX 77258
2	GB TECH LOCKHEED ATTN LUCILLE BORREGO C23C JOE FALCON JR C23C 2400 NASA ROAD 1 HOUSTON TX 77058
6	GDLS 38500 MOUND RD ATTN W BURKE MZ436-21-24 G CAMPBELL MZ436-30-44 D DEBUSSCHER MZ436-20-29 J ERIDON MZ436-21-24 W HERMAN MZ 435-01-24 S PENTESCU MZ436-21-24 STERLING HTS MI 48310-3200

NO. OF COPIES	ORGANIZATION
2	GENERAL RESEARCH CORP ATTN A CHARTERS T MENNA PO BOX 6770 SANTA BARBARA CA 93160-6770
1	GRC INTERNATIONAL ATTN TIMOTHY M CUNNINGHAM 5383 HOLLISTER AVE SANTA BARBARA CA 93111
7	INST OF ADVANCED TECHNOLOGY UNIVERSITY OF TX AUSTIN ATTN S J BLESS J CAZAMIAS J DAVIS H D FAIR T M KIEHNE D LITTLEFIELD M NORMANDIA 4030-2 W BRAKER LN AUSTIN TX 78759
1	INTERNATIONAL RESEARCH ASSOC ATTN D L ORPHAL 4450 BLACK AVE PLEASANTON CA 94566
1	INTERPLAY ATTN F E WALKER 18 SHADOW OAK RD DANVILLE CA 94526
1	ITT SCIENCES AND SYSTEMS ATTN J WILBECK 600 BLVD SOUTH, SUITE 208 HUNTSVILLE AL 35802
1	R JAMESON 624 ROWE DR ABERDEEN MD 21001
1	KAMAN SCIENCES CORP ATTN DENNIS L JONES 2560 HUNTINGTON AVE SUITE 200 ALEXANDRIA VA 22303
7	KAMAN SCIENCES CORP ATTN J ELDER RICHARD P HENDERSON DAVID A PYLES FRANK R SAVAGE JAMES A SUMMERS TIMOTHY W MOORE THY YEM 600 BLVD S SUITE 208 HUNTSVILLE AL 35802
3	KAMAN SCIENCES CORP ATTN SHELDON JONES GARY L PADEREWSKI ROBERT G PONZINI 1500 GRDN OF THE GODS RD COLORADO SPRINGS CO 80907
4	KAMAN SCIENCES CORP ATTN NASIT ARI STEVE R DIEHL WILLIAM DOANE VERNON M SMITH PO BOX 7463 COLORADO SPRINGS CO 80933-7463
1	D R KENNEDY & ASSOC INC ATTN D KENNEDY PO BOX 4003 MOUNTAIN VIEW CA 94040
1	KERLEY PUBLISHING SERVICES ATTN G I KERLEY PO BOX 13835 ALBUQUERQUE NM 87192-3835
2	KTECH CORPORATION ATTN FRANK W DAVIES LARRY M LEE 901 PENNSYLVANIA NE ALBUQUERQUE NM 87110
1	LIVERMORE SOFTWARE TECH CORP ATTN J O HALLQUIST 2876 WAVERLY WAY LIVERMORE CA 94550

NO. OF COPIES ORGANIZATION

1 LOCKHEED MARTIN MISSLE & SPACE
ATTN WILLIAM R EBERLE
PO BOX 070017
HUNTSVILLE AL 35807

3 LOCKHEED MARTIN MISSILE & SPACE
ATTN M A LEVIN ORG 81 06 BLDG 598
M R MCHENRY
T A NGO ORG 81 10 BLDG 157
111 LOCKHEED WAY
SUNNYVALE CA 94088

4 LOCKHEED MISSILE & SPACE CO
ATTN JOHN R ANDERSON
WILLIAM C KNUDSON
S KUSUMI 0 81 11 BLDG 157
J PHILLIPS 0 54 50
PO BOX 3504
SUNNYVALE CA 94088

1 LOCKHEED MISSILE & SPACE CO
ATTN R HOFFMAN
SANTA CRUZ FACILITY
EMPIRE GRADE RD
SANTA CRUZ CA 95060

1 LOCKHEED NASA JSC
SPACE SCIENCE BRANCH
ATTN JAMES HYDE
BOX 58561 MC B22
HOUSTON TX 77258

1 MCDONNELL DOUGLAS
ASTRONAUTICS CO
ATTN B L COOPER
5301 BOLSA AVE
HUNTINGTON BEACH CA 92647

2 ORLANDO TECHNOLOGY INC
ATTN DANIEL A MATUSKA
MICHAEL GUNGER
PO BOX 855
SHALIMAR FL 32579-0855

1 PHYSICAL SCIENCES INC
ATTN PETER NEBOLSINE
20 NEW ENGLAND BUS CTR
ANDOVER MA 01810

NO. OF COPIES ORGANIZATION

3 PHYSICS INTERNATIONAL
ATTN R FUNSTON
G FRAZIER
L GARNETT
PO BOX 5010
SAN LEANDRO CA 94577

1 PRC INC
ATTN J ADAMS
5166 POTOMAC DR #103
KING GEORGE VA 22485-5824

1 RAYTHEON ELECTRONIC SYSTEMS
ATTN R KARPP
50 APPLE HILL DRIVE
TEWKSBURY MA 01876

1 ROCKWELL INTERNATIONAL
ROCKETDYNE DIVISION
ATTN H LEIFER
16557 PARK LN CIRCLE
LOS ANGELES CA 90049

1 ROCKWELL MISSILE SYS DIV
ATTN T NEUHART
1800 SATELLITE BLVD
DULUTH GA 30136

1 SAIC
ATTN MICHAEL W MCKAY
10260 CAMPUS POINT DR
SAN DIEGO CA 92121

1 SHOCK TRANSIENTS INC
ATTN DAVID DAVISON
BOX 5357
HOPKINS MN 55343

2 SIMULATION & ENG CO INC
ATTN ELSA I MULLINS
STEVEN E MULLINS
8840 HWY 20 SUITE 200 N
MADISON AL 35758

2 SOUTHERN RESEARCH INSTITUTE
ATTN LINDSEY A DECKARD
DONALD P SEGERS
PO BOX 55305
BIRMINGHAM AL 35255-5305

NO. OF COPIES ORGANIZATION

5 SRI INTERNATIONAL
ATTN JAMES D COLTON
D CURRAN
R KLOOP
R L SEAMAN
D A SHOCKEY
333 RAVENSWOOD AVE
MENLO PARK CA 94025

2 TELEDYNE BROWN ENGR
ATTN JIM W BOOTH
MARTIN B RICHARDSON
PO BOX 070007 MS 50
HUNTSVILLE AL 35807-7007

1 ZERNOW TECHNICAL SVCS INC
ATTN LOUIS ZERNOW
425 W BONITA AVE SUITE 208
SAN DIMAS CA 91773

1 SUNY STONEYBROOK
DEPT APPL. MATH & STAT.
ATTN J GLIMM
STONEYBROOK NY 11794

ABERDEEN PROVING GROUND

9 DIR, USARL
ATTN: AMSRL-WM, I MAY
AMSRL-WM-BC, A ZIELINSKI
AMSRL-WM-BD,
R PESCE-RODRIGUEZ
A KOTLAR
AMSRL-WM-BE, S HOWARD
AMSRL-WM-MB, G GAZONAS
AMSRL-WM-MC, J M WELLS
AMSRL-WM-T,
W F MORRISON
T W WRIGHT

NO. OF COPIES ORGANIZATION

43 DIR, USARL
ATTN: AMSRL-WM-TA,
W GILLICH
S BILYK
M BURKINS
W BRUCHEY
J DEHN
G FILBEY
W A GOOCH
H W MEYER
E J RAPACKI
J RUNYEON
AMSRL-WM-TB,
R FREY
P BAKER
R LOTTERO
J STARKENBERG
AMSRL-WM-TC,
W S DE ROSSET
T W BJERKE
R COATES
F GRACE
K KIMSEY
M LAMPSON
D SCHEFFLER
S SCHRAML
G SILSBY
B SORENSEN
R SUMMERS
W WALTERS
AMSRL-WM-TD,
S CHOU
A M DIETRICH
J M BOTELER
D DANDEKAR
K FRANK
M RAFTENBERG
A RAJENDRAN
M SCHEIDLER
S SCHOENFELD
S SEGLETES (5 CP)
T WEERASOORIYA
AMSRL-WM-WD,
J POWELL
A PRAKASH

NO. OF COPIES	ORGANIZATION
4	AERONAUTICAL & MARITIME RESEARCH LABORATORY ATTN N BURMAN R WOODWARD S CIMPOERU D PAUL PO BOX 4331 MELBOURNE VIC 3001 AUSTRALIA
1	ABTEILUNG FUER PHYSIKALISCHE CHEMIE MONTANUNIVERSITAET ATTN E KOENIGSBERGER A 8700 LEOBEN AUSTRIA
1	PRB S A ATTN M VANSNICK AVENUE DE TERVUEREN 168 BTE 7 BRUSSELS B 1150 BELGIUM
1	ROYAL MILITARY ACADEMY ATTN E CELENS RENAISSANCE AVE 30 B1040 BRUSSELS BELGIUM
1	BULGARIAN ACADEMY OF SCIENCES SPACE RESEARCH INSTITUTE ATTN VALENTIN GOSPODINOV 1000 SOFIA PO BOX 799 BULGARIA
1	CANADIAN ARSENALS LTD ATTN P PELLETIER 5 MONTEE DES ARSENAUX VILLIE DE GRADEUR PQ J5Z2 CANADA
1	DEFENCE RSCH ESTAB SUFFIELD ATTN D MACKAY RALSTON ALBERTA TOJ 2NO RALSTON CANADA

NO. OF COPIES	ORGANIZATION
1	DEFENCE RSCH ESTAB SUFFIELD ATTN CHRIS WEICKERT BOX 4000 MEDICINE HAT ALBERTA TIA 8K6 CANADA
1	DEFENCE RSCH ESTAB VALCARTIER ARMAMENTS DIVISION ATTN R DELAGRAVE 2459 PIE X1 BLVD N PO BOX 8800 CORCELETTE QUEBEC GOA 1R0 CANADA
1	UNIVERSITY OF GUELPH PHYSICS DEPT ATTN C G GRAY GUELPH ONTARIO N1G 2W1 CANADA
1	CEA ATTN ROGER CHERET CEDEX 15 313 33 RUE DE LA FEDERATION PARIS 75752 FRANCE
1	CEA CISI BRANCH ATTN PATRICK DAVID CENTRE DE SACLAY BP 28 GIF SUR YVETTE 91192 FRANCE
1	CEA/CESTA ATTN ALAIN GEILLE BOX 2 LE BARP 33114 FRANCE
6	CENTRE D'ETUDES DE GRAMAT ATTN SOLVE GERARD CHRISTIAN LOUPIAS PASCALE OUTREBON J CAGNOUX C GALLIC J TRANCHET GRAMAT 46500 FRANCE

NO. OF COPIES ORGANIZATION

2 CENTRE D'ETUDES DE LIMEIL-VALENTON
ATTN CHRISTIAN AUSSOURD
JEAN-CLAUDE BOZIER
SAINT GEORGES CEDEX
VILLENEUVE 94195
FRANCE

3 CENTRE D'ETUDES DE VAUJOURS
ATTN PLOTARD JEAN-PAUL
ERIC BOTTET
TAT SIHN VONG
BOITE POSTALE NO 7
COUNTRY 77181
FRANCE

6 CENTRE DE RECHERCHES
ET D'ETUDES D'ARCUEIL
ATTN D BOUVART
C COTTENNOT
S JONNEAUX
H ORSINI
S SERROR
F TARDIVAL
16 BIS AVENUE PRIEUR DE
LA COTE D'OR
F94114 ARCUEIL CÉDEX
FRANCE

1 DAT ETBS CETAM
ATTN CLAUDE ALTMAYER
ROUTE DE GUERRY BOURGES
18015
FRANCE

1 ETBS DSTI
ATTN P BARNIER
ROUTE DE GUERAY
BOITE POSTALE 712
18015 BOURGES CEDEX
FRANCE

1 FRENCH GERMAN RESEARCH INST
ATTN CHANTERET P-Y
CEDEX 12 RUE DE I'INDUSTRIE
BP 301
F68301 SAINT-LOUIS
FRANCE

NO. OF COPIES ORGANIZATION

5 FRENCH GERMAN RESEARCH INST
ATTN HANS-JURGEN ERNST
FRANCIS JAMET
PASCALE LEHMANN
K HOOG
H LERR
CEDEX 5 5 RUE DU GENERAL
CASSAGNOU
SAINT LOUIS 68301
FRANCE

1 LABORATOIRE DE TECHNOLOGIE DES
SURFACES
ECOLE CENTRALE DE LYON
ATTN VINET P
BP 163
69131 ECULLY CEDEX
FRANCE

1 BATTELLE INGENIEUTECHNIK GMBH
ATTN W FUCHE
DUESSELDORFFER STR 9
ESCHBORN D 65760
GERMANY

1 CONDAT
ATTN J KIERMEIR
MAXIMILIANSTR 28
8069 SCHEYERN FERNHAG
GERMANY

1 DEUTSCHE AEROSPACE AG
ATTN MANFRED HELD
POSTFACH 13 40
D 86523 SCHROBENHAUSEN
GERMANY

1 DIEHL GBMH AND CO
ATTN M SCHILDKNECHT
FISCHBACHSTRASSE 16
D 90552 RÖTBENBACH AD PEGNITZ
GERMANY

NO. OF COPIES ORGANIZATION

4 ERNST MACH INSTITUT
ATTN VOLKER HOHLER
E SCHMOLINSKE
E SCHNEIDER
K THOMA
ECKERSTRASSE 4
D-7800 FREIBURG I BR 791 4
GERMANY

1 EUROPEAN SPACE OPERATIONS CENTRE
ATTN WALTER FLURY
ROBERT-BOSCH-STRASSE 5
64293 DARMSTADT
GERMANY

3 FRAUNHOFER INSTITUT FUER KURZZEITDYNAMIK
ERNST MACH INSTITUT
ATTN H ROTHENHAEUSLER
H SENF
E STRASSBURGER
HAUPTSTRASSE 18
D79576 WEIL AM RHEIN
GERMANY

3 FRENCH GERMAN RESEARCH INST
ATTN HARTMUTH F LEHR
ROLF HUNKLER
ERICH WOLLMANN
POSTFACH 1260
WEIL AM RHEIN D-79574
GERMANY

2 IABG
ATTN M BORRMANN
H G DORSCH
EINSTEINSTRASSE 20
D 8012 OTTOBRUN B MUENCHEN
GERMANY

1 INGENIEURBÜRO DEISENROTH
AUF DE HARDT 33 35
D5204 LOHMAR 1
GERMANY

NO. OF COPIES ORGANIZATION

3 TU CHEMNITZ-ZWICKAU
ATTN I FABER
L KRUEGER
LOTHAR MEYER
FAKULTAET FUER MASCHINENBAU U. VERFAHRENSTECHNIK
SCHEFFELSTRASSE 110
09120 CHEMNITZ
GERMANY

1 TU MÜNCHEN
ATTN E IGENBERGS
ARCISSTRASSE 21
8000 MÜNCHEN 2
GERMANY

2 UNIVERSITÄT PADERBORN
FACHBEREICH PHYSIK
ATTN O SCHULTE
W B HOLZAPFEL
D 33095 PADERBORN
GERMANY

1 BHABHA ATOMIC RESEARCH CENTRE
HIGH PRESSURE PHYSICS DIVISION
ATTN N SURESH
TROMBAY BOMBAY 400 085
INDIA

1 NATIONAL GEOPHYSICAL RESEARCH INSTITUTE
ATTN G. PARTHASARATHY
HYDERABAD-500 007 (A. P.)
INDIA

5 RAFAEL BALLISTICS CENTER
ATTN EREZ DEKEL
YEHUDA PARTOM
G ROSENBERG
Z ROSENBERG
Y YESHURUN
PO BOX 2250
HAIFA 31021
ISRAEL

1 TECHNION INST OF TECH
FACULTY OF MECH ENGNG
ATTN SOL BODNER
TECHNION CITY
HAIFA 32000
ISRAEL

NO. OF COPIES	ORGANIZATION
1	IHI RESEARCH INSTITUTE STRUCTURE & STRENGTH ATTN: TADASHI SHIBUE 1-15, TOYOSU 3 KOTO, TOKYO 135 JAPAN
1	ESTEC CS ATTN DOUGLAS CASWELL BOX 200 NOORDWIJK 2200 AG NETHERLANDS
2	EUROPEAN SPACE AGENCY ESTEC ATTN LUCY BERTHOUD MICHEL LAMBERT POSTBUS BOX 299 NOORDWIJK NL2200 AG NETHERLANDS
4	PRINS MAURITS LABORATORY ATTN H J REITSMA EDWARD VAN RIET H PASMAN R YSSELSTEIN TNO BOX 45 RIJSWIJK 2280AA NETHERLANDS
1	ROYAL NETHERLANDS ARMY ATTN J HOENEVELD V D BURCHLAAN 31 PO BOX 90822 2509 LS THE HAGUE NETHERLANDS
4	HIGH ENERGY DENSITY RESEARCH CTR ATTN VLADIMIR E FORTOV GENADII I KANEL V A SKVORTSOV O YU VOJOBIEV IZHORSKAJA STR 13/19 MOSCOW 127412 RUSSIAN REPUBLIC
1	INSTITUTE OF CHEMICAL PHYSICS ATTN A YU DOLGOBORODOV KOSYGIN ST 4 V 334 MOSCOW RUSSIAN REPUBLIC
3	INSTITUTE OF CHEMICAL PHYSICS RUSSIAN ACADEMY OF SCIENCES ATTN A M MOLODETS S V RAZORENOV A V UTKIN 142432 CHERNOGOLOVKA MOSCOW REGION RUSSIAN REPUBLIC
3	INSTITUTE OF MECH ENGINEERING PROBLEMS ATTN V BULATOV D INDEITSEV Y MESCHERYAKOV BOLSHOY, 61, V.O. ST PETERSBURG 199178 RUSSIAN REPUBLIC
1	INSTITUTE OF MINEROLOGY & PETROGRAPHY ATTN V A DREBUSHCHAK UNIVERSITETSKI PROSPEKT, 3 630090 NOVOSIBIRSK RUSSIAN REPUBLIC
2	IOFFE PHYSICO TECHNICAL INSTITUTE DENSE PLASMA DYNAMICS LABORATORY ATTN EDWARD M DROBYSHEVSKI A KOZHUSHKO ST PETERSBURG 194021 RUSSIAN REPUBLIC
1	IPE RAS ATTN A A BOGOMAZ DVORTSOVAIA NAB 18 ST PETERSBURG RUSSIAN REPUBLIC
2	LAVRENTYEV INST. HYDRODYNAMICS ATTN LEV A MERZHIEVSKY VICTOR V SILVESTROV 630090 NOVOSIBIRSK RUSSIAN REPUBLIC
1	MOSCOW INST OF PHYSICS & TECH ATTN S V UTYUZHNIKOV DEPT OF COMPUTATIONAL MATHEMATICS DOLGOPRUDNY 1471700 RUSSIAN REPUBLIC

NO. OF COPIES ORGANIZATION

1 RESEARCH INSTITUTE OF MECHANICS
NIZHNIY NOVGOROD STATE UNIVERSITY
ATTN A SADYRIN
P.R. GAYARINA 23 KORP 6
NIZHNIY NOVGOROD 603600
RUSSIAN REPUBLIC

1 RUSSIAN FEDERAL NUCLEAR CENTER
ATTN LEONID F GUDARENKO
MIRA AVE., 37
SAROV 607190
RUSSIAN REPUBLIC

1 SAMARA STATE AEROSPACE UNIV
ATTN L G LUKASHEV
SAMARA
RUSSIAN REPUBLIC

1 TOMSK BRANCH OF THE INSTITUTE
FOR STRUCTURAL MACROKINETICS
ATTN V GORELSKI
8 LENIN SQ GSP 18
TOMSK 634050
RUSSIAN REPUBLIC

1 UNIVERSIDAD DE CANTABRIA
FACULTAD DE CIENCIAS
DEPARTMENTO DE FISICA APLICADA
ATTN J AMOROS
AVDA DE LOS CASTROS S/N
39005 SANTANDER
SPAIN

4 DEPARTMENTO DE QUIMICA FISICA
FACULTAD DE CIENCIAS QUIMICAS
UNIVERSIDAD COMPLUTENSE DE
MADRID
ATTN V G BAONZA
M TARAVILLO
M CACERAS
J NUNEZ
28040 MADRID
SPAIN

NO. OF COPIES ORGANIZATION

1 CARLOS III UNIV OF MADRID
ATTN C NAVARRO
ESCUELA POLITEENICA
SUPERIOR
C/. BUTARQUE 15
28911 LEGANES MADRID
SPAIN

1 UNIVERSIDAD DE OVIEDO
FACULTAD DE QUIMICA
DEPARTMENTO DE QUIMICA FISICA Y
ANALITICA
ATTN E FRANCISCO
AVENIDA JULIAN CLAVERIA S/N
33006 - OVIEDO
SPAIN

1 DYNAMEC RESEARCH AB
ATTN ÅKE PERSSON
P.O. BOX 201
S-151 23 SÖDERTÄLJE
SWEDEN

6 NATL DEFENCE RESEARCH EST
ATTN LARS HOLMBERG
ULF LINDEBERG
LARS GUNNAR OLSSON
L HOLMBERG
B JANZON
I MELLGARD
FOA BOX 551
TUMBA S-14725
SWEDEN

2 SWEDISH DEFENCE RSCH ESTAB
DIVISION OF MATERIALS
ATTN S J SAVAGE
J ERIKSON
STOCKHOLM S-17290
SWEDEN

1 K&W THUN
ATTN W LANZ
ALLMENDSSTRASSE 86
CH-3602 THUN
SWITZERLAND

NO. OF COPIES ORGANIZATION

2 AWE
ATTN MICHAEL GERMAN
WAYNE HARRISON
FOULNESS ESSEX SS3 9XE
UNITED KINGDOM

1 CENTURY DYNAMICS LTD
ATTN NIGEL FRANCIS
DYNAMICS HOUSE
HURST RD
HORSHAM
WEST SUSSEX RH12 2DT
UNITED KINGDOM

1 DERA
ATTN I CULLIS
FORT HALSTEAD
SEVENOAKS KENT TN14 7BJ
UNITED KINGDOM

6 DEFENCE RESEARCH AGENCY
ATTN W A J CARSON
I CROUCH
C FREW
T HAWKINS
B JAMES
B SHRUBSALL
CHOBHAM LANE CHERTSEY
SURREY KT16 0EE
UNITED KINGDOM

1 UK MINISTRY OF DEFENCE
ATTN GRAHAM J CAMBRAY
CBDE PORTON DOWN SALISBURY
WITTSHIRE SPR 0JQ
UNITED KINGDOM

1 K TSEMBELIS
SHOCK PHYSICS GROUP
CAVENDISH LABORATORY
PHYSICS & CHEMISTRY OF SOLIDS
UNIVERSITY OF CAMBRIDGE
CAMBRIDGE CB3 0HE
UNITED KINGDOM

NO. OF COPIES ORGANIZATION

2 UNIVERSITY OF KENT
PHYSICS LABORATORY
UNIT FOR SPACE SCIENCES
ATTN PHILIPPE GENTA
PAUL RATCLIFF
CANTERBURY KENT CT2 7NR
UNITED KINGDOM

7 INSTITUTE FOR PROBLEMS IN MATERIALS STRENGTH
ATTN S FIRSTOV
B GALANOV
O GRIGORIEV
V KARTUZOV
V KOVTUN
Y MILMAN
V TREFILOV
3, KRHYZHANOVSKY STR
252142, KIEV-142
UKRAINE

1 INSTITUTE FOR PROBLEMS OF STRENGTH
ATTN G STEPANOV
TIMIRYAZEVSKAYU STR 2
252014 KIEV
UKRAINE

1 INSTITUTE OF PHYSICS
SILESIAN TECHNICAL UNIVERSITY
ATTN E SOCZKIEWICZ
44-100 GLIWICE
UL. KRZYWOUSTEGO 2
POLAND

REPORT DOCUMENTATION PAGE

Form Approved
OMB No. 0704-0188

1. AGENCY USE ONLY *(Leave blank)*	2. REPORT DATE	3. REPORT TYPE AND DATES COVERED
	September 1998	Final, Jun 97 - Jun 98

4. TITLE AND SUBTITLE

The Vibrational Stiffness of an Atomic Lattice

5. FUNDING NUMBERS

PR: 1L162618AH80

6. AUTHOR(S)

Steven B. Segletes

7. PERFORMING ORGANIZATION NAME(S) AND ADDRESS(ES)

U.S. Army Research Laboratory
ATTN: AMSRL-WM-TD
Aberdeen Proving Ground, MD 21005-5066

8. PERFORMING ORGANIZATION REPORT NUMBER

ARL-TR-1757

9. SPONSORING/MONITORING AGENCY NAMES(S) AND ADDRESS(ES)

10.SPONSORING/MONITORING AGENCY REPORT NUMBER

11. SUPPLEMENTARY NOTES

12a. DISTRIBUTION/AVAILABILITY STATEMENT

Approved for public release; distribution is unlimited.

12b. DISTRIBUTION CODE

13. ABSTRACT ***(Maximum 200 words)***

A static-atomic model is described, which may be employed to evaluate the characteristic vibrational stiffness of an atomic lattice, given the pair-wise potential of the constituent atom. Because the vibrational stiffness is directly related to the resultant vibrational frequency spectrum of the lattice, the method may be used to infer the behavior of the characteristic lattice frequency as a function of lattice spacing. The characteristic frequency behavior is sufficient to determine the Grüneisen function, an important thermodynamic parameter relating to thermal behavior of a crystal lattice. The current method computes and utilizes several spring constants derived from a static lattice in order to infer the characteristic vibrational behavior. No atomic dynamics calculations involving either the equations of motion or modal (vibrational) analysis are required. As such, the method generally requires mere seconds of computation on today's generation of desktop workstations. Results indicate that the vibrational stiffness of the lattice is qualitatively distinct from the volumetric stiffness of the lattice, and, furthermore, that the resulting lattice behavior can be described, over a wide region of lattice spacing, by an analytical equation of state in terms of lattice frequency.

14. SUBJECT TERMS

vibrational stiffness, atomic lattice

15. NUMBER OF PAGES

87

16. PRICE CODE

17. SECURITY CLASSIFICATION OF REPORT	18. SECURITY CLASSIFICATION OF THIS PAGE	19. SECURITY CLASSIFICATION OF ABSTRACT	20. LIMITATION OF ABSTRACT
UNCLASSIFIED	UNCLASSIFIED	UNCLASSIFIED	UL